ANALYTIC CALCULATION OF GROUND STATE PROPERTIES OF THE 2D AND 3D ELECTRON GAS

A THESIS SUBMITTED TO

THE GRADUATE SCHOOL OF ENGINEERING AND SCIENCE

OF BILKENT UNIVERSITY

IN PARTIAL FULFILLMENT OF THE REQUIREMENTS FOR

THE DEGREE OF

MASTER OF SCIENCE

IN

PHYSICS

By

Yağmur Katı

June, 2015

Analytic Calculation of Ground State Properties of the 2D and 3D Electron Gas
By Yağmur Katı
June, 2015

We certify that we have read this thesis and that in our opinion it is fully adequate, in scope and in quality, as a thesis for the degree of Master of Science.

Asst. Prof. Dr. Balázs Hetényi(Advisor)

Prof. Dr. Bilal Tanatar

Assoc. Prof. Dr. Hande Toffoli

Approved for the Graduate School of Engineering and Science:

Prof. Dr. Levent Onural
Director of the Graduate School

ABSTRACT

ANALYTIC CALCULATION OF GROUND STATE PROPERTIES OF THE 2D AND 3D ELECTRON GAS

Yağmur Katı
M.S. in Physics
Advisor: Asst. Prof. Dr. Balázs Hetényi
June, 2015

The electron gas (2D and 3D) is a model which consists of interacting electrons moving in a uniform positive background. Its importance stems from the fact that a number of metals behave similarly, it provides the functional used in density functional theory, and that in 2D it can be experimentally realized. Understanding the behavior of this model is of fundamental importance. In this thesis we present an analysis of this model based on the Hypernetted Chain Method in 3D, and 2D. The HNC method is a variational method to calculate the ground state properties of an interacting system, by expressing the ground state energy as a functional of the radial distribution function. Minimizing the energy expression one obtains a zero energy Schrödinger equation for the square root of the radial distribution function. The potential in this equation can include the effects of fermionic or bosonic exchange. We applied this method to charged boson and electron gas in 2D and 3D systems. On the basis of the results of this research, it can be concluded that we obtained very close correlation energy results compared to Monte Carlo, and FHNC results for the density range when r_s is from 0 to 20. This extended range is important for solid state applications.

Keywords: Electron gas, charged boson, quantum Hall effect, Hypernetted Chain Theory, radial distribution function, ground state energy.

ÖZET

İKİ VE ÜÇ BOYUTLU ELEKTRON GAZININ TEMEL DURUM ÖZELLİKLERİNİN ANALİTİK HESAPLAMASI

Yağmur Katı
Fizik, Yüksek Lisans
Tez Danışmanı: Asst. Prof. Dr. Balázs Hetényi
Haziran, 2015

İki ve üç boyutlu elektron gaz modeli, tekdüze pozitif yüklü bir alanda hareket eden etkileşim halindeki elektronlardan oluşur. Birçok metal birbiriyle benzer davranış gösterdiği, DFTde kullanılan fonksiyoneli sağladığı ve iki boyutta hesaplanan sonuçları deneysel olarak da gerçekleştirilebildiği için bu modelin davranışını anlamak temel önem taşımaktadır. Bu çalışma ile sizlere, HNC metodunu kullanarak üç boyutlu ve iki boyutlu sistemlerde elektron gaz modelinin bir analizini sunuyoruz. HNC Metodu, etkileşim halindeki bir sistemin temel durum enerjisini radyal dağılım fonksiyonunun bir fonksiyoneli olarak ele alıp, temel durum özelliklerini hesaplayan varyasyonel bir metoddur. Enerji ifadesi minimize edilirse, radyal dağılım fonksiyonunun karekökü için sıfır enerjili Schrödinger denklemi elde edilir. Bu denklemdeki potansiyel, fermiyonik veya bozonik değişim içerebilir. Biz bu yöntemi iki ve üç boyutlu yüklü bozon ve elektron gazına ve quantum Hall sistemine uyguladık. Bu araştırmanın sonuçlarına dayanarak, katı hal fiziği uygulamalarında önemli olan $0 < rs < 20$ genişletilmiş yoğunluk aralığı için Monte Carlo ve FHNC sonuçlarına çok yakın korelasyon enerjisi sonuçları elde ettiğimizi söyleyebiliriz.

Anahtar sözcükler: Elektron gazı, yüklü bozon gazı, kuantum Hall etkisi, temel durum enerjisi.

Acknowledgement

The author wishes to thank several people. I would like to express my special appreciation and thanks to my advisor Dr. Balázs Hetényi, for encouraging my research and for allowing me to grow as a scientist.

I would also like to thank my committee members, Prof. Bilal Tanatar and Dr. Hande Toffoli for their brilliant comments and suggestions; and I am grateful to Prof. Cemal Yalabık, and Prof. Atilla Aydınlı for their generous guidance and support.

I am hugely indebted and throughly grateful to Sinan Gündoğdu for his precious help and support during the time it has taken me to finalize this thesis.

Finally I would like to extend my deepest gratitude to my family for all of the sacrifices that they have made on my behalf.

Contents

List of Figures

List of Tables

Chapter 1

Introduction

After science has stepped to quantum mechanics from classical mechanics, nanoscopic examination of matter has attracted extreme interest. The physical problems which include large number of interacting particles that is related to quantum mechanics are named in general as quantum many body problems [1]. The treated problems in this thesis are the 2D and 3D electron liquid systems. We have studied the radial distribution function and ground state energy calculation of two and three dimensional electron liquids by the method of Kallio. We additionally tried the method for two and three-dimensional boson systems too.

The outline of the thesis is as follows. In the second chapter we concisely introduce some background concepts to gain a clear perspective to the thesis: Jellium Model, Wigner-Seits radius, particle density and Coulomb interaction are defined, radial distribution function and static structure factor are discussed, and an outline of the description of a quantum many body system is given to show the systematic approach of the hypernetted chain method (HNC) that we have used in this study.

In Chapter 3 we present the HNC Method aimed to investigate the distribution of electrons and the energies of some simple models. We introduce how the method

is developed via the cluster diagrams in Sec. 3.1. Then, the founding of HNC/0 method, and its iteration process is exhibited in Sec. 3.2. Since, perturbation theory only works for high electron densities (free electron gas), new methods like coupled cluster method and variational methods were developed to solve the problem of strong correlation [2]. One of them is the Fermi hypernetted chain theory (FHNC) which is described in Sec. 3.3. In this method, one deals with four highly nonlinear differential equations to find the ground state properties of a Fermi liquid system. Also, it offers a hard and not exact way to evaluate the elementary diagrams which are represented in Sec. 3.1. Therefore, in 1996, Kallio and Piilo [3] offered a new technique to count the elementary diagrams in a much simpler and exact way. This method, explained in Sec. 3.4, is basically using the HNC/0 method which is modified for fermions to investigate the ground-state properties of many-body fermionic systems.

In Chapter 4, the iterative schemes, the codes with explanations and the results of the calculations for 2D and 3D electron systems are presented. We tried initially for 3D charged bosons in Sec 4.1. Then, we moved our calculation to 2D charged bosons in Sec 4.2. We defined the problems in detail, presented our results, and then compared them with other results in the subsections of each section. In Sec 4.3, we produced the results for 3D free electron gas, and in the following section we moved to 2D electron gas system to calculate the same properties with a fixed scheme for their specific case.

Chapter 2

Background

The theoretical studies on electron liquids had an important role in the improvements on novel materials and modern electronic devices [1]. Considering solid state applications, it is preferred to solve the many body problems by assuming the distribution of electrons is homogeneous. Such a model is the Jellium Model defined in Sec. 2.1. In a many body system, the investigation of the properties of the materials is easier by using the particle density instead of calculating electron-electron interactions for each electron pair. For this reason, we assume a homogenous electron gas with positive background, and investigate its distribution and energy.

Our approximations are:
1) Three body correlations between electrons are neglected.
2) Jellium model is used.
3) Variational approach is used.
4) The Euler-Lagrange equation that we handle is a Schrödinger-like equation. Hence, we assume that we have a Schrödinger equation with zero energy, and its probability is the radial distribution function of the system.
5) Before the iterative calculation process, we presume that the Coulomb potential of the system is zero. This is to build up the fermionic correction term in the Schrödinger-like equation.

First, I would like to introduce the crucial concepts that are needed to be understood before dealing with the interacting electron gas problems.

2.1 Jellium Model

The Jellium Model is known as the homogenous electron gas with a uniform positive background. Scientists are able to study the interaction effects by this model, since it eliminates the effects coming from the periodic crystal potential. In order to reach this homogenous case experimentally, scientists prepare a clear and smooth environment in which electrons move freely and interact only among themselves. Hence, the analytic and experimental results can be compared in this model.

2.1.1 Particle Density and Wigner-Seitz Radius

Many elemental metals and semiconductors can be used for 2D and 3D electron liquid studies. Metals are an example of 3D case since their electrons are able to move freely, due to the almost spherical surface of conducting electrons which is called the Fermi sphere. Every metal has a specific electron density which can be defined by the number r_s. The Wigner-Seitz radius (r_s) is the dimensionless radius of the sphere that encloses one electron if we take average in a homogenous environment. The r_s value multiplied by Bohr radius gives the actual radius of the imaginary sphere of one electron in units of Å. Bohr radius can be defined as:

$$a_0 = \frac{\hbar^2}{me^2} = 0.529\text{Å}. \tag{2.1}$$

The metallic r_s range is roughly between 1.8 to 6 [1, p. 7-8]. However, by using doped metals one can change the electron density of the metal. To control the electron density, we can use dopant concentration as a variable. In those systems the Coulomb interaction formula changes from $\frac{e^2}{r}$ into $\frac{e^2}{\epsilon r}$ where ϵ is the

static dielectric constant. Experimentalists prefer pure semiconductors due to the disorder problems caused by dopant atoms. Pure semiconductors are at zero temperature.

Density of particles in the system can be expressed in terms of r_s and Bohr radius (a_0) for one, two and three dimensional systems as follows [1, p. 17] :

$$\frac{1}{n} = \begin{cases} \frac{4\pi}{3}(r_s a_0)^3 & \text{3D} \\ \pi(r_s a_0)^2 & \text{2D} \\ 2r_s a_0 & \text{1D.} \end{cases} \tag{2.2}$$

2.2 Coulomb Interaction

The Coulomb interaction between two electrons is $v_c(r) = \frac{e^2}{r}$ in Gaussian units for both 2D and 3D systems. To define the Coulomb potential in k space, one takes its Fourier transform, and the result is as follows:

$$v_q = \begin{cases} \frac{4\pi e^2}{q^2} & \text{3D} \\ \frac{2\pi e^2}{q} & \text{2D.} \end{cases} \tag{2.3}$$

In the very high density range such that $r_s \to 0$, Coulomb potential between particles can be neglected due to the dominance of the kinetic energy. We use this fact as a first approximation in our calculations of highly dense systems. By this way, we are able to set a clear analytic method, explained in Chapter 3, to solve for the ground state energy and radial distribution function. Then, we add the contribution of the Coulomb potential to the induced interaction of the system so that the results become reasonable in the r_s range from 0 to 20. It is a useful density range for most solid state applications.

2.3 Radial Distribution Function

Radial distribution function describes the relative behavior of particles, and can be defined as the distribution of electrons about any electron if the average is taken over the motion of the particles [4, p. 60]. It gives significant clues about the system studied. For instance, in order to calculate the ground state energy of a many particle system, we need to obtain its exact radial distribution function. Radial distribution function takes into account the two, three, and more particle correlations. For the high density systems, we can neglect three and more body interactions. The radial distribution function for only two body correlations is called pair distribution function. It is defined as the probability per unit volume that an electron is at r given that there is one at $r = 0$. The spin of the electron has crucial importance on the $g(r)$ of the system. There are two types of $g(r)$ if the electron gas is spin-unpolarized: $g_{\uparrow\uparrow}(r) = g_{\downarrow\downarrow}(r)$ and $g_{\uparrow\downarrow}(r) = g_{\downarrow\uparrow}(r)$. For instance, $g_{\uparrow\downarrow}(r)$ means the probability per volume such that the electron at r has spin-up whereas the center electron has spin-down. These pair distribution functions give the average state of the electrons. In order to show the calculation of the radial distribution function, we start with a Slater Determinant:

$$\psi_{\lambda_1,\lambda_2\ldots\lambda_N}(r_1, r_2 \ldots r_N) = \begin{vmatrix} \phi_{\lambda_1}(r_1) & \phi_{\lambda_1}(r_2) & \ldots & \phi_{\lambda_1}(r_N) \\ \phi_{\lambda_2}(r_1) & \phi_{\lambda_2}(r_2) & \ldots & \phi_{\lambda_2}(r_N) \\ \vdots & \vdots & \ddots & \vdots \\ \phi_{\lambda_N}(r_1) & \phi_{\lambda_N}(r_2) & \ldots & \phi_{\lambda_N}(r_N) \end{vmatrix}$$

where λ_j stands for jth state. Its square gives the N-particle density matrix. However, we need only two particle density matrix to define the pair distribution function of N particles. Therefore, it is found by integrating N-particle density over all in two space coordinates:

$$g_{ss'}(r_1, r_2) = v^2 \int d^3r_3 d^3r_4 \ldots d^3r_N |\psi_{\lambda_1,\lambda_2\ldots\lambda_N}(r_1, r_2 \ldots r_N)|^2, \tag{2.4}$$

where v is the fixed volume [4, p. 301]. We can sum over all possible distribution

wave functions by assuming that one-electron orbitals(ϕ_{λ_j}) are orthogonal:

$$g_{ss'}(r_1, r_2) = \frac{v^2}{N(N-1)} \sum_{\lambda_i, \lambda_j} \begin{vmatrix} \phi_{\lambda_i}(r_1) & \phi_{\lambda_i}(r_2) \\ \phi_{\lambda_j}(r_1) & \phi_{\lambda_j}(r_2) \end{vmatrix}^2 .$$

We can define the one-electron functions as plane waves:

$$\phi_\lambda(r) = \frac{\chi_s}{\sqrt{v}} e^{ik\cdot r}, \tag{2.5}$$

where χ_s stands for the spin functions. Since the radial distribution function defines the orbital section, the average of the spin functions is taken as: $\langle \chi_\uparrow \chi_\uparrow \rangle = 1, \langle \chi_\uparrow \chi_\downarrow \rangle = 0$, etc. For this two spin conditions, $g(r)$ can be calculated as:

$$\begin{aligned} g_{\uparrow\downarrow}(r_1 - r_2) &= \frac{1}{N(N-1)} \sum_{k_1,k_2} (|e^{ik_1\cdot r_1 + ik_2\cdot r_2}|^2 + |e^{ik_1\cdot r_2 + ik_2\cdot r_1}|^2) \\ &= \frac{2}{N(N-1)} \left(\frac{N}{2}\right)^2 = \frac{1}{2}, \end{aligned} \tag{2.6}$$

$$\begin{aligned} g_{\uparrow\uparrow}(r_1 - r_2) &= \frac{1}{N(N-1)} \sum_{k_1,k_2} (|e^{ik_1\cdot r_1 + ik_2\cdot r_2} + e^{ik_1\cdot r_2 + ik_2\cdot r_1}|^2) \\ &= \frac{2}{N(N-1)} \sum_{k_1,k_2} [1 - e^{i(k_1 - k_2)\cdot(r_1 - r_2)}] \\ &= \frac{1}{2}[1 - \Lambda(r_1 - r_2)^2], \end{aligned} \tag{2.7}$$

$$\text{where } \Lambda(r) = \frac{2}{N} \sum_k [1 - e^{ik\cdot r}]. \tag{2.8}$$

The sum in the Eq. (2.8) is calculated over occupied states. As it is shown in Eq. (2.6), the pair distribution function for the antiparallel spin case ($g_{\uparrow\downarrow} \equiv g_{\downarrow\uparrow}$) equals to $\frac{1}{2}$. In the parallel spin case, λ(r) can be calculated as:

$$\lambda(r) = \frac{2}{n_0} \int d^3k \frac{e^{ik\cdot r}}{(2\pi)^3} n_k = \frac{3}{r{k_F}^3} \int_0^{k_F} k \sin(kr) dk = \frac{3}{rk_F} j_1(rk_F). \tag{2.9}$$

One can see the pair distribution functions for parallel and antiparallel spins in the Fig. 2.1. Therefore, the total radial distribution function which varies from 0 to 1 can be expressed as the sum of these two conditions:

$$g(r) = g_{\uparrow\uparrow}(r) + g_{\uparrow\downarrow}(r). \tag{2.10}$$

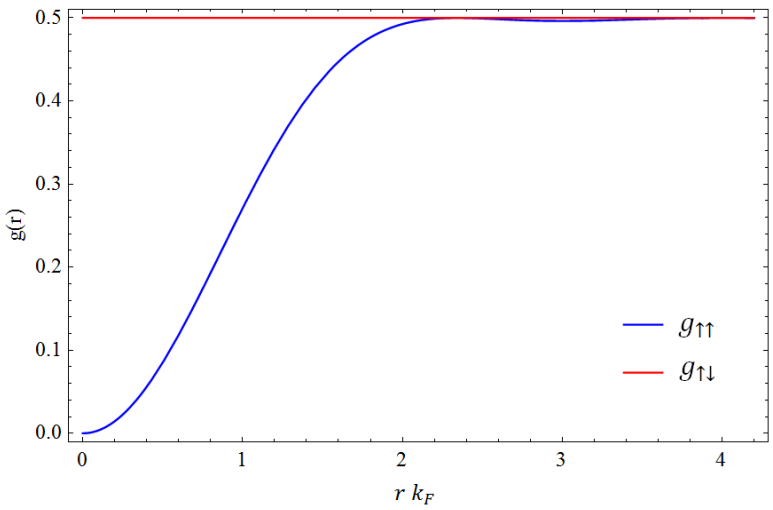

Figure 2.1: The pair distribution functions for parallel and antiparallel spin conditions are found by Hartree-Fock approximation. The blue line represents the $g(r)$ for parallel spins, and the red line represents $g(r)$ for antiparallel spins. The functions are defined in [4, p. 309].

The definition is the same if the center electron is spin-down.

The pair distribution function has two remarkable features. First one is the normalization rule of $g(r)$:

$$n_0 \int d^3r[g(r) - 1] = -1. \tag{2.11}$$

Second is one can calculate the Coulomb energy if the $g(r)$ of the system is known:

$$E_C = \frac{e^2 n_0}{2} \int d^3r \frac{g(r) - 1}{r}. \tag{2.12}$$

2.3.1 Static Structure Factor

Structure factor can be found experimentally by the examination of scattering of the x-rays, and electron or neutron beams from the semiconductor crystals. Thus, the radial distribution function can be determined numerically by the relation

between $S(k)$ and $g(r)$:

$$\begin{aligned} g(r) - 1 &= \frac{1}{n} \int d^3k \frac{e^{-ik\cdot r}}{(2\pi)^3} [S(k) - 1], \\ S(k) - 1 &= n \int d^3r e^{-ik\cdot r} [g(r) - 1]. \end{aligned} \tag{2.13}$$

Likewise the radial distribution function, static structure factor ($S(k)$) approaches unity as k becomes large.

2.4 Description of a Quantum Many Body System

It is challenging to solve the many body Schrödinger Equation in highly dense systems. Due to having many particles in a small area or volume, there will be too many matrix elements so one cannot use the regular perturbative methods and solve them. For this reason, high correlations in short range interactions must be inserted into the wave function initially. We can denote the trial wave function as ψ_T which is used for N particles in the system:

$$\psi_T(1 \dots N) = F(1 \dots N)\phi(1 \dots N), \tag{2.14}$$

where F is the operator factor which represents correlations. It is symmetric under the exchange of particles, and ϕ is the totally symmetric wave function for the free gas that does not take into account the interactions. The ground state means all particles are in their lowest energy state such that $\phi(1 \dots N) = \Omega^{-N/2}$. The function ϕ is considered as the Slater determinant for fermions:

$$\phi(1 \dots N) = \det |\psi_{\alpha i}(j)|. \tag{2.15}$$

Since the function ϕ is for the noninteracting free gas, the single particle wave function $\psi_{\alpha i}$(j) is taken as plane wave:

$$\psi_{\alpha i}(j) = \frac{1}{\Omega^{1/2}} e^{ik_{\alpha_i}\cdot r_j} \sigma(j), \tag{2.16}$$

where σ can be spin-up $|\uparrow\rangle$ or spin-down $|\downarrow\rangle$. Hence, the degeneracy is 2 for unpolarized systems, and 1 for polarized systems. In the thermodynamic limit,

the volume which determines the boundary conditions goes to infinity. Now that the trial wave function is specified, it can be used to get more information about the many particle solid state system. In the variational approach, initially, a trial wave function must be chosen. Through calculating the expectation value of the Hamiltonian of the system, the upper bound to the ground state energy can be found. The following variational method (Hypernetted Chain/0 Method) to evaluate the ground state energy holds for a bosonic many particle system. Since the wave function of a system is symmetric for bosons and antisymmetric for fermions, the calculations are much easier for the bosonic case. The trial wave function must be chosen carefully in order to use the variational approach efficiently. Therefore, the Jastrow correlation wave function (f_2) is selected for two body correlations for the following reasons: It is zero or nearly zero if the distance between two particles is less than the interval of the repellent part of the potential. It approaches unity when the distance is large enough, to take no account of correlation effect. Then, the free parameters of the Jastrow correlation function can be found by minimization of the energy so that the optimum trial function can be established:

$$\frac{\delta}{\delta f}\frac{\langle\Psi_J|H|\Psi_J\rangle}{\langle\Psi_J|\Psi_J\rangle} = 0. \tag{2.17}$$

Here, one can find the expectation value of the Hamiltonian through Monte Carlo methods by handling the integrals in the energy equation directly. Monte Carlo is a numeric method which gives exact results for the trial wave function. For this reason, we will use the recorded results of Monte Carlo for our trial systems as a check. In our calculations we use hypernetted-chain approximation, a more analytical method. Before founding the trial wave function, we should calculate the expectation value of the Hamiltonian of the many body system. For this, we perform the cluster expansion of the integrals and sum up the terms systematically by the aid of diagrammatic notation. Initially, we can calculate the expectation value of the potential energy:

$$\frac{\langle V\rangle}{N} = \frac{1}{N}\frac{\langle\Psi_J|\sum_{i<j}V(r_{ij})|\Psi_J\rangle}{\langle\Psi_J|\Psi_J\rangle} = \frac{N(N-1)}{2N}\frac{\langle\Psi_J|V(r_{12})|\Psi_J\rangle}{\langle\Psi_J|\Psi_J\rangle}. \tag{2.18}$$

Since we have chosen two particles out of N particles, we have to perform the integrals over $r_3, r_4 \dots r_N$:

$$\begin{aligned}\frac{\langle V\rangle}{N} &= \frac{N-1}{2}\frac{\int dr_1 \dots dr_N \Psi_J^*(r_1, r_2 \dots r_N)\Psi_J(r_1, \dots r_N)V(r_{12})}{\int dR|\Psi|^2} \\ &= \frac{n^2}{2N}\int dr_1 dr_2 V(r_{12})\left(\frac{N(N-1)}{n^2}\frac{\int dR_{12}|\Psi_J|^2}{\int dR|\Psi_J|^2}\right),\end{aligned} \tag{2.19}$$

where $dR_{12} = dr_3 dr_4 \dots dr_N$. In Eq. (2.19) we notice that the radial distribution function coincides with the second term in the integral:

$$g(r_1 - r_2) = \frac{N(N-1)}{n^2}\frac{\int dR_{12}|\Psi_J(r_1, \dots, r_N)|^2}{\int dR|\Psi_J(r_1, \dots, r_N)|^2}. \tag{2.20}$$

Hence, we can display the potential energy as:

$$\frac{\langle V\rangle}{N} = \frac{n}{2}\int dr V(r)g(r). \tag{2.21}$$

The expectation value of the kinetic energy is found similarly:

$$\frac{\langle T\rangle}{N} = -\frac{1}{N}\sum_{i=1}^{N}\frac{\hbar^2}{2m}\frac{\langle\Psi_J|{\nabla_i}^2|\Psi_J\rangle}{\langle\Psi_J|\Psi_J\rangle} = -\frac{\hbar^2}{2m}\frac{\langle\Psi_J|{\nabla_1}^2|\Psi_J\rangle}{\langle\Psi_J|\Psi_J\rangle}. \tag{2.22}$$

It is calculated by A. Polls and F. Mazzanti through the Jackson Feenberg Identity. The detailed solution is in [2, p. 59,60], and the final result is

$$\frac{\langle T\rangle}{N} = -\frac{n}{2}\frac{\hbar^2}{2m}\int dr g(r)\nabla_r^2 \ln f(r), \tag{2.23}$$

where $f(r)$ is the Jastrow function. Consequently, the expectation value of the Hamiltonian per particle of a many body system can be written as:

$$e = \frac{E}{N} = \frac{n}{2}\int dr g(r)\left[V(r) - \frac{\hbar^2}{2m}\nabla_r^2 ln f(r)\right]. \tag{2.24}$$

The ground state wavefunction of a Bose system can be defined in the exponential form:

$$\Psi_0(r_1, \dots, r_N) = \exp\left[\frac{1}{2}\chi(r_1, \dots, r_N)\right]. \tag{2.25}$$

In the Eq. (2.25), χ can be decomposed into its components as:

$$\chi_R(r_1, \dots, r_N) = \sum_{n=1}^{N}\sum_{i_1,\dots,i_n} u_n(r_{i_1}, \dots, r_{i_n}), \tag{2.26}$$

where n is the number of interacting bodies, and u is the function of them. By denoting 2.26 into 2.25 the Feenberg ansatz equation can be found:

$$\Psi_0(r_1, \ldots, r_N) = \exp\left[\frac{1}{2}\sum_{i<j}^{N} u_2(r_{ij}) + \frac{1}{2}\sum_{i<j<k} u_3(r_i, r_j, r_k) + \ldots\right]. \tag{2.27}$$

The equation can also be represented as:

$$\Psi_0(r_1, \ldots, r_N) = \prod_{i<j} f_2(r_{ij}) \prod_{i<j<k} f_2(r_i, r_j, r_k \ldots), \tag{2.28}$$

where $f_n = e^{u_n/2}$. Now, since we assume that we are in a highly dense system of particles, the many body interactions which include three and more particles can be ignored. Thus, it is reasonable to choose the following Jastrow wave function which considers only two-body correlations as the first guess of the bosonic wave function:

$$\Psi_J(r_1, \ldots, r_N) = \prod_{i<j} f_2(r_{ij}). \tag{2.29}$$

As stated before, the Jastrow function approaches unity as the distance between the two bodies approaches infinity due to the cluster property.

$$f^{(2)}(r \to \infty) \to 1. \tag{2.30}$$

Chapter 3

Hypernetted Chain Method

3.1 Definition

The hypernetted-chain (HNC) method is a variational method which was developed as an alternative to the field theoretical approach to cope with strong correlations in many-body systems. It offers an analytical and systematic way to improve the ground-state wave function [3] from first principles, and gives a satisfactory description for Bose and Fermi systems with strong interactions, where the perturbation theoretical method often fails. The HNC method is first developed in 1959 by Leeuwen et al. [5] for classical liquid systems to understand the thermo fluctuations of many particle systems at finite temperature, and it is studied for classical systems mostly in 60s and 70s. After the developments in quantum mechanics, HNC theory was also applied to quantum liquid systems to understand quantum fluctuations at zero temperature in highly correlated Boson systems such as Helium. In this thesis, we will take only the quantum applications of this theory into consideration. The method works accurately for homogenous quantum many-body fluids in the thermodynamic limit at 0 K. By the aid of the HNC method, one can find the ground-state properties of interacting systems, such as ground-state energy, the radial distribution function, and the static structure factor. An interacting system includes correlations between two, three

or more particles, hence there occur multidimensional integrals in the definition of radial distribution function. The multidimensional integrals are known as cluster functions. HNC uses a special schematic representation technique to deal with these type of cluster integrals and makes the problem analytically solvable.

In Sec. 2.4, we showed that the radial distribution function is necessary to calculate the total energy of a many particle system as summarized by Eq. (2.24). Now, our aim is to clarify the description of the radial distribution function which is given in Eq. (2.20) by defining the many-particle wave function in terms of the Jastrow function as in Eq (2.29). Thereby, the pair distribution function can be written as follows:

$$g(r) = \frac{N(N-1)}{n^2} \frac{\int \prod_{i<j} f_2^2(r_{ij}) dR_{12}}{\int \prod_{i<j} f_2^2(r_{ij}) dR}. \tag{3.1}$$

In order to solve the equation easily, we will introduce the cluster function $h(r) = f_2^2 - 1$ which goes to zero as the distance between particles approaches infinity.

$$g(r) = \frac{N(N-1)}{n^2} \frac{\int \prod_{i<j} (h(r)+1) dR_{12}}{\int \prod_{i<j} (h(r)+1) dR}. \tag{3.2}$$

After applying power expansion, g(r) becomes:

$$g(r) = \frac{N(N-1)\Omega^{-N}}{n^2\Omega^{-N}} \frac{\int dR_{12}(1 + \sum_{i<j} h(r_{ij}) + \sum_{i<j,k<l} h(r_{ij})h(r_{kl}) + \cdots)}{\int dR(1 + \sum_{i<j} h(r_{ij}) + \sum_{i<j,k<l} h(r_{ij})h(r_{kl}))}, \tag{3.3}$$

where Ω^{-N} stands for the total volume of the system with N particles. The sum can be converted to its integral form. Here is an example:

$$\int dR_{12}\Omega^{-N+2} \sum_{i=3}^{N} h(r_{1i})h(r_{i2}) = n \int dr_j h(r_{1j})h(r_{j2}). \tag{3.4}$$

In Eq. (3.4), the reason that the sum starts from $i = 3$ to N is that we chose two external particles ($i = 1, 2$) and look for the internal particle that integrates these two external particles. Because the number of remaining particles is $N - 2$, the volume factor becomes $\Omega^{-(N-2)}$. We take the integral with respect to $dR_{12} = dr_3, dr_4, ..., dr_N$, and sum up the multiplication of two $h(r)$ functions for $N - 2$ different points. This sum can be written as an integral simply by taking infinitesimal points. At the right hand side of Eq. (3.4), n is the density of

particles, and the integral is taken with respect to r_j, where j stands for the internal particle.

The multidimensional integrals including one or more cluster functions are called cluster terms (see Eq. 3.3). As the amount of the integrated coordinates increases, the calculation of the cluster terms become more complicated. We will introduce the diagrammatic notation of cluster integrals to clarify the problem. This notation leads us to realize the integrals with the same result and the essential cancellations between the infinite sets of cluster functions so that the problem becomes solvable. Below are the rules of the diagrammatic analogy:

- One diagram can represent many cluster integrals.
- Every internal (integrated) particle corresponds to a solid circle.
- Every external (not integrated) particle corresponds to an open circle.
- Every $h(r_{ij})$ function connecting the particles i and j, is represented as dashed line.

The difference in the integrated coordinates does not change the result of the integral. For instance, in Eq. (3.4), the integral of $h(r_{15})h(r_{25})$ and $h(r_{18})h(r_{28})$ gives the same outcome, and they are delineated by the same diagram. We can represent the integral in the Eq. (3.4) as in Fig. 3.1(a) where 1 and 2 are the particles which are integrated. Further, the internal point, j, does not change the yield of the integral. The diagram notation of the cluster function

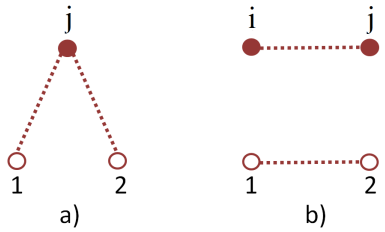

Figure 3.1: The representation of cluster functions. a) for two integrated particles, b) for two nonintegrated particles, reproduced from [2, p. 64].

$h(r_{12})\frac{(N-2)(N-3)}{2\Omega}\int dr_{ij}h(r_{ij})$ is depicted in the Fig. 3.1(b) as an example. Here, r_{ij} is the distance between particles i and j. In this cluster function, $h(r_{12})$ is not involved in the integral, since the coordinates 1 and 2 are not integrated. The factor $(N-2)(N-3)$ is multiplied due to the selection of two points from the number of possible choices. Also, the term is divided by Ω that comes from the change of variables, such that $\int dr_1 dr_2 \to \int dR dr = \Omega \int dr$ where $r = r_1 - r_2$ and $R = (r_1 + r_2)$. Additionally, the term is multiplied by $1/2$ due to the fact that the result is the same if the label of the particles i and j are exchanged. The other diagrams can be evaluated in this way. We note that the particles should be close enough to consider their correlation effect, since $f(r \to \infty) \to 1$ corresponds to $h(r \to \infty) \to 0$. This means the diagrams including more lines contribute less to the radial distribution function. Therefore, we can use the less complicated diagrams to approximate $g(r)$. The diagrams can be classified as linked or unlinked. Linked diagrams have only one way to connect the particles which are represented as open or closed circles in the diagram. However, there are some not connected parts in the unlinked diagrams. The unlinked and linked diagrams can be seen in the Fig. 3.2. Linked diagrams are grouped as reducible and irreducible. In reducible diagrams there is an articulation point which is a circle pointed with an arrow. It separates the diagram into different parts [2, p. 65]. It is hard to decide which of those diagrams should be kept for the radial distribution. Thankfully, there is a theorem which states that we can consider only the cluster functions corresponding to irreducible diagrams in the numerator of Eq. (3.3), since the reducible and unlinked diagrams on the numerator are cancelled by the denominator up to the order $1/N$ [6]. Thus, one can simply define the pair distribution function as the sum of topologically distinct irreducible diagrams, as in Eq. (3.12). The irreducible diagrams are divided into composite diagrams labeled as X, and simple diagrams which are separated to nodal and elementary diagrams labeled as N and E, respectively. In a diagram, if there is only one line from one external point to another, then the internal points on this line are denoted as nodes. In Fig. 3.2, it can be seen that elementary diagrams have no node whereas nodal diagrams have at least one node.

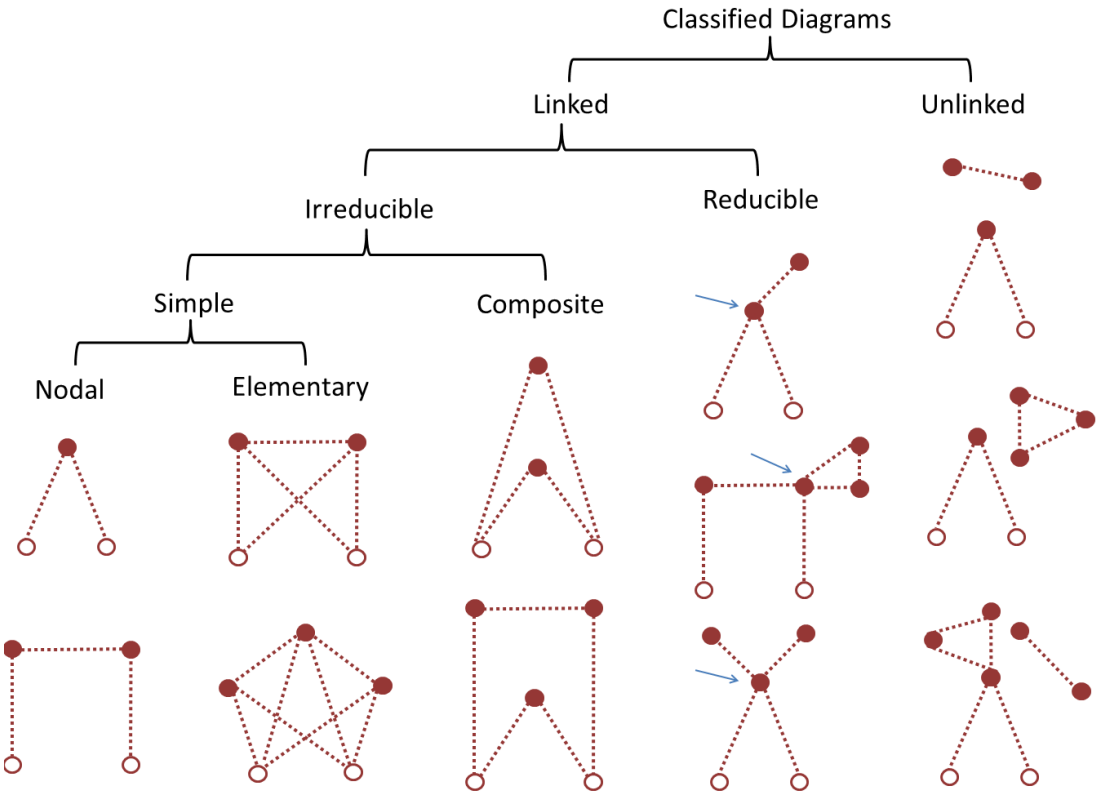

Figure 3.2: The notations of linked, unlinked, reducible, and irreducible diagrams, reproduced from [2, p. 66].

The cluster diagrams are formed by the aid of convolution and algebraic products. The integrals of functions $a(r_{ik})$ and $b(r_{kj})$ are represented as convolution products:

$$n(a(r_{ik})|b(r_{kj})) \equiv n \int dr_k a(r_{ik}) b(r_{kj}), \tag{3.5}$$

where k is the nodal point, because it is the only connection between the two external points: i and j. In addition to this, the algebraic product of the two functions produces a composite $i-j$ subdiagram. Herein, we can form the HNC equation, but omit the contribution of elementary diagrams initially. $N(r)$ is the sum of the nodal diagrams, and we take solely the subset of them found by the first iteration. In order to build the chain, first the convolution product of $N(r)$ and $h(r)$ is carried out. Thus, we obtain all nodal diagrams with the exception of the convolution product of two $h(r)$ functions [2, p. 68]. This situation is exhibited in the Fig. 3.3. Hence, the selected set of diagrams satisfies the following equation:

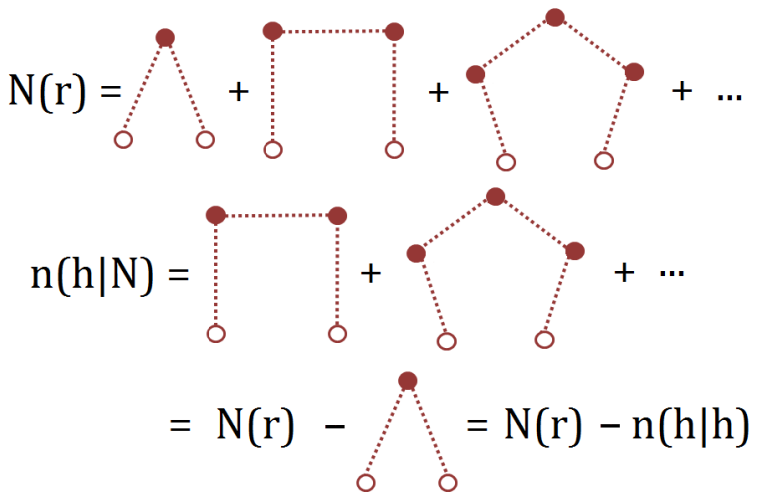

Figure 3.3: The diagrammatic representation of the operation between nodal functions and convolution products, reproduced from [2, 66].

$$n(h(r_{ij})|N(r_{j2})) = N(r_{12}) - n(h(r_{ij})|h(r_{j2})). \tag{3.6}$$

By this way, $N(r)$ is constructed, and it is used to establish composite diagrams. Composite diagrams include at least two $1-2$ subdiagrams. The sum of these subdiagrams consists of $\frac{N^n(r)}{n!}$ terms where n is the number of $1-2$ subdiagrams. The terms are divided by n! in order not to count the same terms due to the symmetry. Hence; in the thermodynamic limit, the sum can be written as

$$\sum_{n=2}^{\infty} \frac{N^n}{n!} = e^N - N(r) - 1. \tag{3.7}$$

If we multiply $\exp[N(r)]$ with $h(r)$ to obtain more composite diagrams, we get the same diagrams except the term e^Nh(r). Thus, the sum of all the composite diagrams which has the notation $X(r)$ equals:

$$X(r) = e^N - N - 1 + (e^N)h(r). \tag{3.8}$$

Now, we can place the equation $h(r) = f^2(r) - 1$ into Eq. (3.8), and find $X(r)$ as:

$$X(r) = {f_2}^2(r)e^{N(r)} - N(r) - 1. \tag{3.9}$$

Here, we see the results of the first iteration in the HNC scheme: $X(r)$ and $N(r)$. We place the newly found $X(r)$ into the Eq. (3.8) instead of $h(r_{ij})$:

$$n(X(r_{1j})|N(r_{j2})) = N(r_{12}) - n(X(r_{1j})|X(r_{j2})). \tag{3.10}$$

By this equation, $N(r)$ can be found directly, and used in Eq. (3.9) to find the new $X(r)$. This is the basic HNC iteration process between equations (3.8) and (3.9) that lasts until the convergence is reached. Since we did not take the elementary diagrams, it is named as HNC/0 method. However, now we can add the contribution of elementary diagrams to the term $X(r)$:

$$X(r) = f_2^2(r)e^{[N(r)+E(r)]} - N(r) - 1. \tag{3.11}$$

As stated before, $g(r)$ is the total sum of the topologically distinct diagrams which titled as nodal, elementary and composite diagrams.

$$g(r) = 1 + X(r) + N(r) = f_2^2(r)e^{N(r)+E(r)}. \tag{3.12}$$

The iteration scheme for the HNC Method accounting elementary diagrams is generated by the equations (3.10) and (3.11). Since Fourier transform converts convolutions to algebraic products, it aids to solve $N(r)$ in Eq. (3.10).

$$N(k) = \frac{X^2(k)}{1 - X(k)}. \tag{3.13}$$

At this point, we will define the Fourier transform as:

$$a(k) = n \int dr e^{ik\cdot r} a(r), \tag{3.14}$$

where n is the particle density. Static structure factor, defined in Sec. 2.3.1, can also be expressed in terms of cluster functions by using Eq. (3.11) due to the Fourier relationship described in Eq. (2.13):

$$\begin{aligned} S(k) - 1 &= \mathcal{F}[g(r) - 1] \\ &= \mathcal{F}[(1 + X(r) + N(r)) - 1] \\ &= X(k) + N(k). \end{aligned} \tag{3.15}$$

Now, we can define the functions N and X in the k space in terms of the static structure factor:

$$\begin{aligned} N(k) &= \frac{(S(k) - 1)^2}{S(k)}, \\ X(k) &= \frac{S(k) - 1}{S(k)}, \end{aligned} \tag{3.16}$$

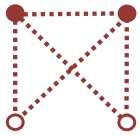

Figure 3.4: An elementary diagram sample with four point structure.

where $X(r)$ may not include the contribution of elementary diagrams depending on the HNC process. The elementary diagrams consist of at least four points, and the simplest one is represented in the Fig 3.4. It is not possible to express sum of the infinite set of elementary diagrams in a closed form. At this point, one should consider making an approximation. One approximation is counting no elementary diagrams and this approach is named HNC/0, as mentioned before. On the other hand, one can consider only the four points elementary diagram (see Fig 3.4) denoted as E_4, and this approach is labeled as HNC/4. However; if we use $g(r) - 1$ in place of $h(r)$ in the HNC/4 approach, the elementary diagram contributions can be built on E_4 after each iteration, because $g(r)$ consists of the sum of all the diagrams. Hereby, we can do a better approximation to the exact result. Also, we note that HNC/0 method, which is iterated on $g(r) - 1$ instead of $h(r)$, gives a good approximation for the bosonic case in the high density limit. Nevertheless; in the fermion case, the contribution coming from the elementary diagrams is not negligible. This case will be treated in the Sec. 3.3.

3.2 Minimization of the Energy

As defined before in Eq. (2.24), the energy per bosonic particle depends on $g(r)$ and f_2(r) :

$$e = \frac{n}{2} \int dr g(r) \left[V(r) - \frac{\hbar^2}{2m} \nabla_r^2 ln f(r) \right]. \tag{3.17}$$

Here, $V(r)$ equals the Coulomb potential for the systems we studied. To solve this equation, the radial distribution function and Jastrow function can be defined in terms of each other if we remember Eq. (3.11).

$$g(r) = 1 + X(r) + N(r) = f_2^2(r) e^{N(r)+E(r)}. \tag{3.18}$$

Here, we can take the functional derivative of the energy with respect to $g(r)$ or $f(r)$ to minimize the energy and find the optimum trial function. We thought that it is better to get rid of $f(r)$ term by defining it in terms of $g(r)$ so that we do not need to find the Jastrow correlation function. Instead, we will use a reasonable $g(r)$ as a first guess for the studied many body system. In this manner, we can define our energy per particle in terms of $g(r)$. The detailed solution of the following process is expressed in Appendix A. First, we do the HNC/0 approximation to solve the energy minimization problem handily, that means $E(r)$ is taken as zero in Eq. (3.11). After Fourier transforming $N(k)$, which is defined in Eq. (3.13), and taking the log of both sides we get:

$$\ln f(r) = \frac{1}{2}\left[\ln g(r) - \frac{1}{(2\pi)^3 n}\int \frac{(S(k)-1)^2}{S(k)} e^{ik\cdot r} dk\right]. \tag{3.19}$$

Then, we insert Eq. (3.19) into Eq. (3.17), and find the total energy per particle as:

$$e = \frac{n}{2}\int dr g(r) v_c(r) - \frac{\hbar^2}{8m}\frac{1}{(2\pi)^3 n}\int dk k^2 \frac{(S(k)-1)^3}{S(k)} - \frac{n}{2}\frac{\hbar^2}{4m}\int dr g(r)\nabla^2 \ln g(r). \tag{3.20}$$

It is easier to do the variational derivative with respect to $\sqrt{g(r)}$ instead of taking the functional derivative with respect to $g(r)$. Here, I should note that the condition for optimization is equivalent for both trials. $\sqrt{g(r)}$ can be denoted as G so that the energy minimization with respect to G is:

$$\begin{aligned} 0 &= \frac{\delta e(n)}{\delta G} \\ &= \frac{\delta}{\delta G}\left[\frac{n}{2}\int dr G^2(r) v_c(r) - \frac{\hbar^2}{8m}\frac{1}{(2\pi)^3 n}\int dk k^2 \frac{(S(k)-1)^3}{S(k)} + \frac{\hbar^2}{2m} n \int dr (\nabla G(r))^2\right]. \end{aligned} \tag{3.21}$$

In the Appendix A, we have taken the functional derivative step by step by using the Parseval identity. Then, we find the so called zero energy Schrödinger like equation with the wave function G(r):

$$\frac{\delta}{\delta G}(e(n)) = 0 \quad \Rightarrow \quad -\frac{\hbar^2}{m}\nabla^2 G(r) + [v_c(r) + W_B(r)]G(r) = 0. \tag{3.22}$$

Here, W_B(r) is the bosonic induced potential which is defined in k space as:

$$W_B(k) = -\frac{\hbar^2 k^2}{4m}\left[\frac{(S(k)-1)}{S(k)}\right]^2 (2S(k)+1). \tag{3.23}$$

In the energy equation we have the static structure factor $S(k)$. Since we can study the energy minimization in the momentum space, we can do the functional derivative with respect to $S(k)$:

$$\frac{\delta e(n)}{\delta S(k)} = 0 \qquad \Rightarrow \qquad S(k) = \frac{1}{\sqrt{\frac{2}{\epsilon(k)} V_{ph}(k)}}, \tag{3.24}$$

where $\epsilon(k)$ is the kinetic energy, and $V_{ph}(k)$ is the Fourier transform of the particle-hole effective interaction which can be represented as:

$$V_{ph}(r) = g(r)v_c(r) + W_B(r)[g(r) - 1] + \frac{\hbar^2}{m}|\nabla\sqrt{g(r)}|^2. \tag{3.25}$$

The iteration process to find the optimum $g(r)$ is summed up by the above equations (3.22 - 3.25). At first, one should use a reasonable first guess for $g(r)$, and corresponding $S(k)$. First, we place $S(k)$ into the Eq. (3.23) and Fourier transform it to find W_B(r). Then, we put $g(r)$ and $W_B(r)$ into the Eq. (3.25), so that $V_{ph}(r)$ is calculated. By Fourier transformation, one can find $V_{ph}(k)$ which will be put into the Eq (3.24) so that the new $S(k)$ is found. The iteration process should continue until there will be no observable change in $g(r)$. Then, the energy per particle can be obtained by replacing the last $g(r)$ and $S(k)$ into the energy equation for a bosonic system.

3.3 Variational Approach for Fermi Systems

If the many particle system consists of fermions, the contribution coming from the elementary diagrams become so significant that we cannot eliminate them as we do in the HNC/0 approximation. In the Fermi Hypernetted Chain Method (FHNC), one must take at least four point elementary diagrams. After several steps, we will introduce only the compact definition of the radial distribution

function which is obtained in detail in [2, p 102-111].

$$\begin{aligned} g(r) =& f_2^2(r)\exp[N_{dd}(r)+E_{dd}(r)] \\ & [1-\frac{l^2(rk_F)}{v}+N_{ee}(r)+E_{ee}(r)+[N_{de}(r)+E_{de}(r)]^2 \\ & +2[N_{de}(r)+E_{ee}(r)]v[N_{cc}(r)+E_{cc}(r)]^2 \\ & +2l(rk_F)[N_{cc}(r)+E_{cc}(r)]]. \end{aligned} \tag{3.26}$$

Here, $l(x)$ is the Slater function, v is the spin degeneracy, and a, b, c, d notations stand for the four points of E_4. A sample diagram of four point elementary function was represented in Fig. 3.4 in which the dashed lines corresponds to the cluster functions in the integral. Because this integral is too complicated to be evaluated exactly, and easily; a more effective method is required. Hence, in 1996, Kallio and Piilo [3] have introduced a novel technique which offers an exact way to count elementary diagrams for fermions. In this technique, we can use the simple HNC/0 method with an additional correction term that accounts for the contribution of elementary diagrams. As well as it offers an exact way to count elementary functions, it reduces the time of the computation.

3.4 HNC/0 Approximation For Fermions

The HNC/0 method for fermions has developed in 1995 by Kallio et. al [7]. The method basically assume that there is a zero energy Schrödinger equation which is satisfied by the probability amplitude $\psi = \sqrt{g(r)}$. The potential part of the Schrödinger equation consists of the Coulomb potential ($v_c(r)$) and the induced interaction potential denoted as $W(r)$. The induced interaction, which is explained in Eq. (3.22) for the bosonic case, includes one additional term, $W_F(r)$, for the fermionic case. It is the key part of the novelty of this method, since $W_F(r)$ is the correction term to account the elementary diagrams exactly. This new term is found analytically by using the fact that Coulomb potential can be neglected at an extreme electron density situation. By the aid of the fermionic correction term, we are able to use the HNC/0 method for fermions such that the hardness and the time spent are thoroughly low if compared to the

FHNC method. At first, we will introduce the iteration process of Kallio that is solved for the bosonic case, and then move the discussion to fermions. In this way, we will use a defect function R to solve the highly nonlinear zero energy equation (3.22). The iteration process is described in detail as follows: First, we will define the most realistic radial distribution function for the handled many body problem. Here, note that the wave function of the zero energy Schrödinger Equation is equal to $\sqrt{g(r)}$. Then, the pair distribution function can be put into the following defect function:

$$R(r) = -\frac{\nabla^2(g-1)}{2} + \frac{\nabla^2\psi}{\psi}. \tag{3.27}$$

By this way, the new S(k) can be found via placing the Fourier transformed R(r) into the following equation:

$$S(k) = \frac{1}{\sqrt{1 + \frac{4\gamma}{k^4} - \frac{4}{k^2}R(k)}} \tag{3.28}$$

with γ is $4\pi n/a_0$. a_0 is the Bohr radius defined in Eq. (2.1) . Next, the new g(r) is obtained through the relation between $S(k)$ and $g(r)$ if we recall Eq. (2.13):

$$g(r) - 1 = \frac{1}{n}\int d^3k \frac{e^{-ik\cdot r}}{(2\pi)^3}[S(k)-1] = F^{-1}[S(k)-1]. \tag{3.29}$$

This is the iteration scheme for bosons that is introduced in Sec. 3.2. Actually, this is the same HNC/0 process, but there is a little difference in their ways to solve the nonlinear zero energy Schrödinger equation and we show their equivalence in Appendix B. Now, we can move our discussion to many-body fermion case. At this point, we add a fermionic correction term to the induced potential $W_B(r)$ in the Eq. (3.22):

$$-\frac{\hbar^2}{m}\nabla^2\psi + (v_c + W_B + W_F)\psi = 0. \tag{3.30}$$

As mentioned before, $W_F(r)$ can be found by the assumption that we deal with an extremely dense fermion system so that the Coulomb potential can be neglected:

$$-\frac{\hbar^2}{m}\nabla^2\psi + (W_B + W_F)\psi = 0. \tag{3.31}$$

Hence, the W_F is able to be found directly by putting W_B into the Eq. (3.31):

$$W_F(k) = -\frac{\hbar^2k^2}{4m}\left[\frac{(S_F(k)-1)}{S_F(k)}\right]^2(2S_F(k)+1) + F\left[\frac{\hbar^2}{m}\frac{\nabla^2\psi}{\psi}\right], \tag{3.32}$$

where $\psi = \sqrt{g_F}$. This time new $S(k)$ is calculated in the form

$$S(k) = \frac{1}{\sqrt{1 + 4\gamma/k^4 + (4/k^2)\left[(m/\hbar^2)W_F(k) - R(k)\right]}}. \tag{3.33}$$

The iteration process is applied between Eq. (3.27) and Eq. (3.33). After the convergence is reached, one may consider calculating the energy of the system per fermion. The potential energy of a many particle system is calculated in two ways. One may use $g(r)$ or $S(k)$ and get the same result for the interaction energy:

$$\begin{aligned} \frac{V}{N} &= \frac{n}{2}\int d^3r[g(r) - 1]v_c(r) \\ &\equiv \frac{1}{2(2\pi)^3}\int d^3k[S(k) - 1]\frac{4\pi e^2}{k^2}. \end{aligned} \tag{3.34}$$

In our calculations, we used both methods to compare and verify our energy values.

Chapter 4

Two and Three Dimensional Many Body Systems

We have investigated the ground state properties of charged bosons and electrons including the calculation of ground state energy, radial distribution function, and static structure factor. Bosons are particles with integer spin values, and they obey Bose-Einstein statistics. As a bosonic system we used composite boson system properties, and investigated the ground state behavior of 3D and 2D charged bosons. Fermions obey Fermi-Dirac statistics and have half-integer spin, and they are restricted by Pauli exclusion principle. Fermions include electrons, protons and neutrons. As fermions, we studied 3D, and 2D electron liquid systems.

4.1 3D Charged Boson Gas

4.1.1 Definition

The charged boson fluid has been usually treated as a basic model of quantum many-body systems in statistical mechanics. Even though the Bose fluid has no

applications in the real world, it has attracted much interest as a model for superconductors, after the discovery of high temperature superconductivity. There is also a possibility to experimentally generate them using metals such as palladium or vanadium highly doped with deuterium [8]. Additionally, this model has a relevance to astrophysics [9, 10, 11] in the expression of pressure-ionized helium in cold degenerate stellar matter.

We first tried our method on many body charged boson fluid, since it is the fundamental quantum system to which the hypernetted-chain method can be applied. Charged boson gas is a many particle system which has only the Coulomb interaction between its bosonic particles. We applied the main hypernetted-chain method to calculate the pair distribution function, static structure factor, and ground state energy of the bosonic system. Also, we investigated how the distribution function and energy depends on r_s. Additionally, we compared our results with Diffusion Monte Carlo (DMC) and HNC results.

4.1.2 The Algorithm

For the three dimensional Bose gas, it is known that the radial distribution function equals to 1 for the noninteracting case. Since we do not include the Coulomb potential which is the only interaction between charged boson particles; the probability to find another boson at any distance from our reference particle equals to 1. Therefore, $g_B(r) = 1$. Due to the Fourier transform relationship between $g(r)$ and $S(k)$ in Eq. (3.29), the corresponding static structure factor of that radial distribution function will be 1 too. Here is the step by step description of the iterative scheme of 3D Bose gas which is summarized in Sec. 3.2, and explained in Sec. 3.4:

1 Initially, we use dimensionless variables to make our calculations simpler:

$$r/r_0 \to r, \qquad k \cdot r_0 \to k \tag{4.1}$$

where $r_0 = r_s \cdot a$ is the radius of a sphere that encloses one particle on

average. The defect function is defined as:

$$R(r) = -\frac{\nabla^2(g-1)}{2} + \frac{\nabla^2\psi}{\psi}, \tag{4.2}$$

where $\psi = \sqrt{g(r)}$. To find the defect function, we take the Laplacian of $g(r)$ in the Eq. (4.2):

$$\Delta g = \frac{1}{r^2}\frac{\partial}{\partial r}(r^2\frac{\partial g}{\partial r}) \tag{4.3}$$

We write $r_s = 0$ in the code for the first calculation, since we are starting with the noninteracting case or high density limit.

The defect function can be calculated by using $g_B(r) = 1$, and $S_B(k) = 1$. After one iteration, we will use the new $g(r)$ and $S(k)$ to calculate $R(r)$.

2 One can find the new $S(k)$ through taking the Fourier transform of $R(r)$, and placing it into the equation:

$$S(k) = \frac{1}{\sqrt{1 + \frac{4\gamma}{k^4} - \frac{4}{k^2}R(k)}} \tag{4.4}$$

where $\gamma = 4\pi n/a$. Here, a is the Bohr radius defined in Eq. (2.1), and n is the density of bosons:

$$n = \frac{3}{4\pi}\frac{1}{(r_s a)^3} \tag{4.5}$$

3 By inserting new $S(k)$ function into the following equation, one can find new g(r):

$$\begin{aligned} g(r) - 1 = \mathcal{F}^{-1}[S(k)-1] &= \frac{1}{n}\int d^3k \frac{e^{-ik\cdot r}}{(2\pi)^3}[S(k)-1] \\ &= -\frac{4\pi}{3}(r_s a)^3 \int dk \frac{k^2(S-1)}{(2\pi)^3}\int_1^{-1} d(\cos\theta) e^{ikr\cos\theta}\int_0^{2\pi} d\phi \\ &= \frac{2(r_s a)^3}{3\pi}\int dk[S(k)-1]k^2\frac{\sin(kr)}{kr} \\ &\equiv \frac{2}{3\pi}\int dk[S(k)-1]k^2\frac{\sin(kr)}{kr} \end{aligned} \tag{4.6}$$

4 Now, we return to step 1, and insert the new definitions of $g(r)$ and $S(k)$ into the equations (4.2), and (4.3). This whole procedure should be repeated until the convergence is reached. Fig. 4.1 shows that the radial distribution

function converges to a certain form after 60 iterations for a 0.1 increase in r_s. Although normally, 10 to 20 iterations are enough to reach convergence, the iteration number is 60 for this specific case. This is because we used a mix of the new $g(r)$ and the previous $g(r)$. For the 3D boson case when r_s is between 0 to 1, the new radial distribution function can be taken as:

$$g(r) = \frac{4 \cdot g_{prev}(r) + g_{new}(r)}{5} \tag{4.7}$$

Mixing a function is a known numerical tool used in iterative algoritms to reduce errors, and it can be adjusted for different r_s values. We have plotted the convergence scheme for all of the calculations to determine the mixing rate by checking if the convergence is smooth. In Fig. 4.1, a dot corresponds to the value of the integral: $\int dr|g_{after}(r) - g_{before}(r)|$. We stopped the computation when this value become smaller than 1×10^{-7}. We plotted the last $g(r)$ and its corresponding $S(k)$ functions for different r_s values in Fig. 4.2.

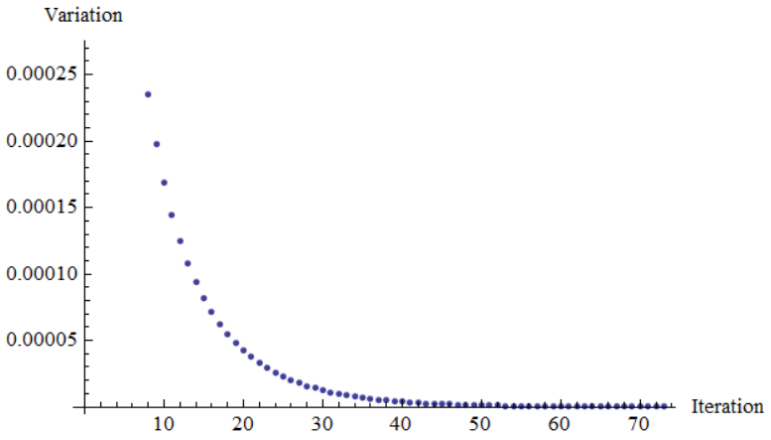

Figure 4.1: The plot of the convergence of the radial distribution function

5 After finding the interacting state $g(r)$, we calculate the potential energy of the system first:

$$\frac{V}{N} = V(r_s) = \frac{n}{2} \int d^3r(g(r) - 1)v_c(r) \tag{4.8}$$

where $v_c(r) = e^2/r$. Another way of finding the potential energy is to apply the integration in k space by using the interacting $S(k)$:

$$V(r_s) = \frac{1}{2(2\pi)^3} \int d^3k[S(k) - 1]\frac{4\pi e^2}{k^2} \tag{4.9}$$

From Eq. (4.9), it is obvious that potential energy depends on the value r_s. We used both ways (4.8, 4.9) to calculate $V(r)$ to check our results. Now, we can find the ground state energy by coupling constant integration, using Eq. (4.8) :

$$E_{GS} = \frac{1}{{r_s}^2} \int_0^{r_s} dr_s' r_s' V(r_s') \tag{4.10}$$

In our code, the upper limit of the integration is r_s as seen in Eq. (4.10). For $r_s = 5$, the potential energy is computed from $r_s = 0$ to $r_s = 5$ by 0.1 steps. Then, $V(r_s)$ is interpolated in order to have a continuous function that will be integrated with respect to the variable r_s. Hence, we could calculate the total energy for $r_s = 5$. The same calculation is done for different r_s values between $0 - 20$ by placing the aimed r_s value into the Eq. (4.10).

4.1.3 Results and Analysis

The plot of the radial distribution function as a function of $r/r_s a$ can be seen in the Fig. 4.2.

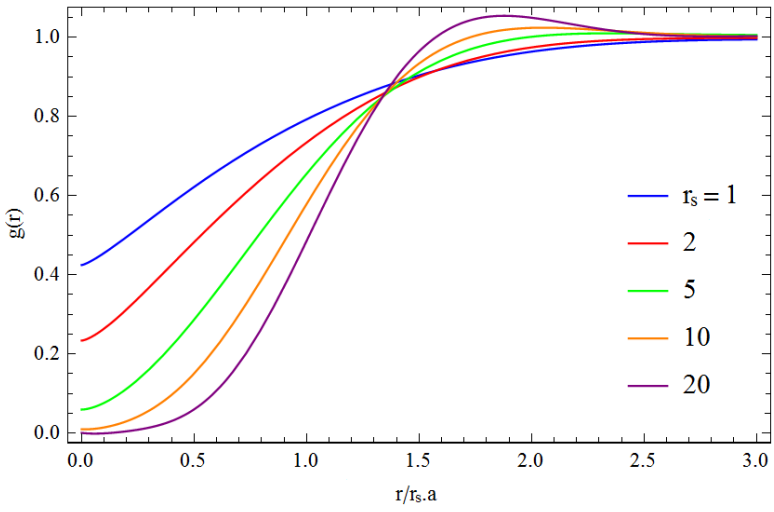

Figure 4.2: Radial distribution function versus $r/r_s a$ for 3D Boson gas

Due to the definition of radial distribution function, and the fact that we take $g(r)$

as the probability amplitude of the Schrödinger-like equation; we can assume that it acts like the probability of finding a particle at r distance from the reference particle. As expected, Fig. 4.2 shows that $g(r = 0)$ approaches to zero as r_s increases, since the probability of finding two particles at the same place decreases with the decreasing density.

The corresponding static structure factor versus kr_0 is plotted for different r_s values which is shown in the Fig. 4.3.

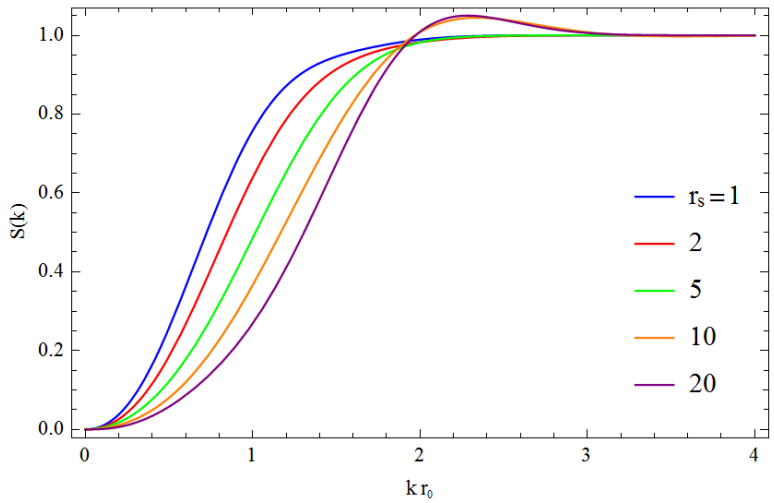

Figure 4.3: Static structure factor versus kr_0 for 3D Bose gas

The static structure factor takes values from 0 to 1 for all of our calculations. Its reason can be easily verified via Eq. (4.4). As exhibited in Eq. (4.9), this function is also used to find the total energy. Since there is no Fermi level for bosons, we do not include the Fermi energy part in our energy definition. After the computations, we recorded the ground state energy results for different r_s values, and then compared with the results with other methods. In Table 4.1, one can see that our results are very close to the exact DMC results, although we did not take three body correlations into account. We also compared our results with the results of Apaja and Halinen who uses the same HNC/0 Method including triplet correlations. The energy comparison from Table 4.1 shows that there is not a significant difference between our results and theirs even though our method is much simpler. This part of the study is important, since it demonstrates that our iteration method and code works very well, and we are ready to convert our

r_s	E_g^{pres}	E_g^{HNC}	E_g^{DMC}
0.1	-4.46523	-4.48857	
1	-0.76618	-0.77675	-0.77664
2	-0.44841	-0.45203	-0.45192
3	-0.32523		
5	-0.21432	-0.21657	-0.216420
10	-0.12135	-0.12144	-0.121353
20	-0.06659	-0.06664	-0.066639

Table 4.1: Ground state energies of the 3D charged boson fluid in Ry at several densities. E_g^{pres} present calculation, DMC results from Ref. [12], HNC results from Ref. [8].

scheme into other bosonic and fermionic cases. Moreover, we calculated a highly nonlinear differential equation by an analytically based method via iterations, and mathematical operations. The integrals and derivatives during the iteration process are evaluated numerically.

4.2 2D Charged Boson Fluid

4.2.1 Definition

As mentioned Sec. 4.1, the fluid of 2D charged bosons has not been experimentally realized. However, its basic model has importance for real world applications due to being a 2D many particle system which has Coulomb potential between its particles. Moreover, the recent studies on quantum Hall effect show that the electron liquid in strong magnetic field acts like a quantum many-body system. To understand the basic principles of the quantum Hall effect, one can initially consider the ground state of a 2D charged boson in the absence of an external magnetic field.

4.2.2 The Algorithm

In this part of the study, we have calculated the ground state energy of 2D charged Bose gas. We have converted the iterative scheme of three-dimensional system into two-dimensional including integrations, Fourier transforms, and the definition of particle density. A short description of the iteration process can be seen in the following:

1 Here, we use the same unitless system which holds for 3D Bose gas. For the first iteration, $g_B(r)$ and $S_B(k)$ are equal to 1.

The particle density for the 2D Bose gas:

$$n = \frac{1}{\pi(r_s a)^2} \tag{4.11}$$

By using the equivalence of two HNC methods which is mentioned in Sec. 3.4 and solved in Appendix C; the two-dimensional γ is found as:

$$\gamma = \frac{2\pi n}{a} = \frac{2}{{r_s}^2 a^3} \tag{4.12}$$

The defect function $R(r)$ is defined in Eq. (4.2). While we are calculating $R(k)$, we have changed the definition of Laplacian and Fourier transform from 3D to 2D in the code. The laplacian is taken in polar coordinates:

$$\Delta g = \frac{1}{r}\frac{\partial}{\partial r}(r\frac{\partial g}{\partial r}) \tag{4.13}$$

2 Now, we can find the new $S(k)$ by placing the functions γ and $R(k)$ into the equation:

$$S(k) = \frac{1}{\sqrt{1 + \frac{4\gamma_{2d}}{k^3} - \frac{4}{k^2}R(k)}} \tag{4.14}$$

3 To find new $g(r)$, one can use the Fourier transform relationship between

$S(k)$ and $g(r)$:

$$\begin{aligned} g(r) - 1 = \mathcal{F}^{-1}[S(k) - 1] &= \frac{1}{n} \int d^2k \frac{e^{-ik\cdot r}}{(2\pi)^2}[S(k) - 1] \\ &= \pi(r_s a)^2 \int dk \frac{(S-1)}{(2\pi)^2} k \int_0^{\pi} d\theta e^{ikr\cos\theta} \\ &= \frac{(r_s a)^2}{2} \int dk[S(k) - 1]kJ_0[kr] \\ &\equiv \frac{1}{2} \int dk[S(k) - 1]kJ_0[kr] \end{aligned} \tag{4.15}$$

4 As stated in Sec. 4.1.2, we use the mixed $g(r)$ in step 1, and continue the iteration process until the value of the integral: $\int dr|g_{after}(r) - g_{before}(r)|$ become less than 1×10^{-7}.

5 The potential energy can be found as follows:

$$\begin{aligned} V(r_s) = \frac{n}{2} \int d^2r(g-1)v_c(r) &= \frac{1}{2\pi(r_s a)^2} \int r dr d\theta (g-1)\frac{e^2}{r} \\ &= \frac{e^2}{(r_s a)^2} \int dr(g-1) = \frac{e^2}{2a}\left(\frac{2}{{r_s}^2 a} \int dr(g-1)\right) \\ &\equiv \left[\frac{2}{r_s} \int dr(g-1)\right] \mathrm{Ry} \end{aligned} \tag{4.16}$$

It is defined in terms of Ry, the Rydberg constant, which equals to $e^2/2a$. Then, we can find the total energy by the same way decribed in the step 5 in Sec. 4.1.2.

4.2.3 Results and Analysis

In Fig. 4.4 the radial distribution function versus $r/r_s a$ is plotted for different boson densities. As stated previously, we initiated the iteration from the high density limit $r_s \to 0$, where $g(r) = 1$, to the lower densities. When r_s increases, the contribution of the Coulomb interaction on the ground state energy also increases. At the high density limit, the kinetic part of the energy expression dominates over the potential part. Consequently, the Coulomb interaction between particles does not contribute a significant amount to the total energy of

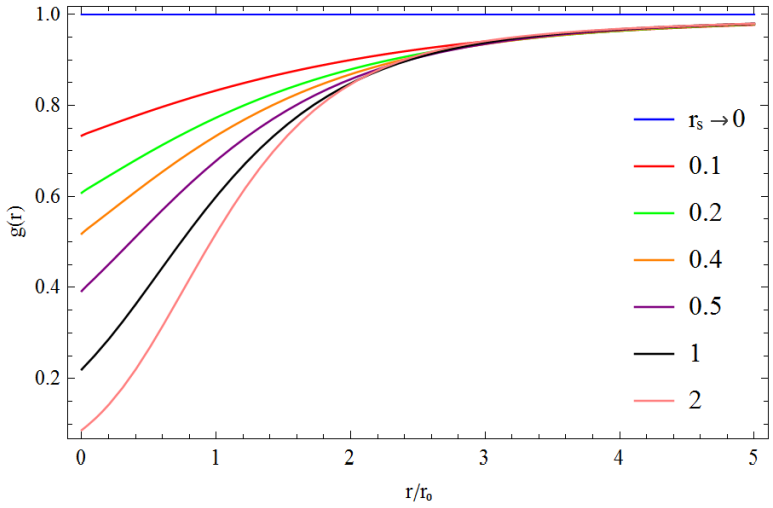

Figure 4.4: Radial distribution function versus $r/r_s a$ for 2D Boson gas in high density regime.

the system. That is why we can assume that Coulomb force is switched off for very low r_s values. Oppositely, when r_s becomes higher, the potential part of the energy expression dominates. Hence, the Coulomb potential become more important at higher r_s values as you can see in Fig. 4.5. Despite of the fact that

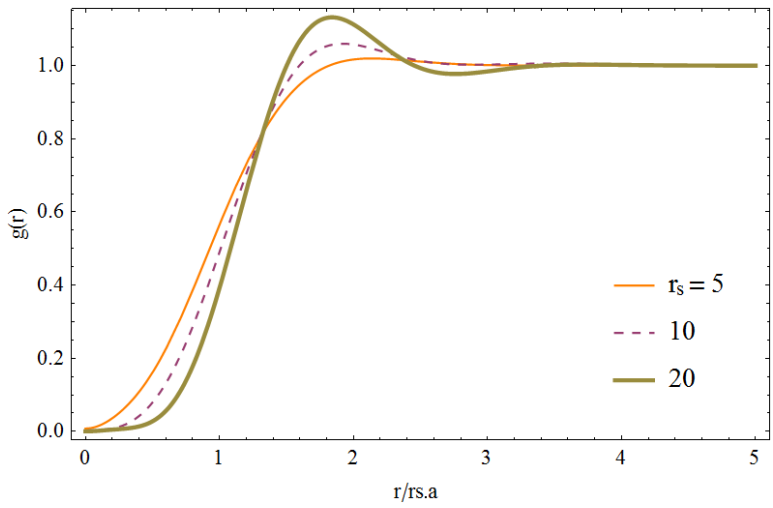

Figure 4.5: Radial distribution function versus $r/r_s a$ for 2D Boson gas

r_s must be much higher than 20 in the case of a Wigner crystal, we can still see the effect of the crystal state in Fig. 4.5. As we know, the plot of a Wigner crystal must have many peaks in its $g(r)$ plot. Nevertheless, since we are still

far away from that case, we only see a small peak on the function while we are approaching to the crystal state. That is why we observe a higher peak for a higher r_s value in Fig. 4.5.

The numerical results for 2D bosons are given in Table 4.2. Actually, we can

r_s	E_c^{pres}	E_c^{STW}	E_c^{STLS}
0.1	-5.8322		
1	-1.1337	-1.1062	-0.1103
2	-0.6640	-0.6631	-0.6484
3	-0.4872	-0.4818	-0.5965
4	-0.3841	-0.3796	
5	-0.3174	-0.3133	-0.3078
10	-0.1732	-0.16685	-0.1724
20	-0.0916	-0.086024	

Table 4.2: Ground-state energy results for two-dimensional charged boson gas in Ry. STW results are from Ref. [13] using a parametrized variational wave function, STLS results from Ref. [14] calculated using the STLS scheme.

safely say that three-body correlations are more important for 2D systems than 3D systems due to the fact that the probability to find three particles close to each other is higher for the particles which are restricted in two dimensions. Although our results for the ground-state energies are not "exact" due to neglecting triplet correlations, they are very close to the other numerical data in the various calculations which are summarized in Table 4.2.

4.3 3D Spin Unpolarized Electron Gas

4.3.1 Definition

Electron gas is a model consisting of electrons interacting by Coulomb forces. Owing to the article published in 1957 by Gell-Mann and Brueckner [15] on the correlation energy of electron gas at high densities, there has been a growing

interest to understand the properties of electron gas on positive uniform background. The studies on homogenous electron gas are particularly significant in condensed matter physics [16, 17] due to the fact that electron gas can be used as a simple reference model for electronic structure calculations.

As it is mentioned in Chapter 1, there are several methods to solve many electron systems, and we handled FHNC which provides an analytical solution of a variational theory based on Jastrow function. In Chapter 3, we explained how FHNC is developed, and the problems related to elementary diagrams. In Sec. 3.4, we introduced the improvement on FHNC by Kallio et al. who propose a simpler way to achieve more accurate results. In this work, our main aim is to contribute to the understanding of the electron gas, and to generalize the usage of this simple method to solve other Fermi systems such as two-dimensional electron liquids. For this reason, we first reproduced the results found by Kallio, and then applied this method for 2D electron gas. In Sec. 4.1.3, we had mentioned that DMC method provides exact results for bosons, so that we could check our analytical results against them. However; for fermions, DMC results are not exact because of the Slater determinant nodes. Nevertheless, one can still compare their results with other methods to evaluate the accuracy of their method.

4.3.2 The Algorithm

In Sec. 3.4, we have described the novel method of Kallio and Piilo, and explained the trick they used to find the elementary diagrams between equations (3.30, 3.32). Here, we will show how this method is applied for unpolarized 3D electron gas by discussing the iteration scheme step by step:

1 First, we use dimensionless variables to simplify our problem.

$$r/r_s a \to r, \qquad k/k_F \to k \tag{4.17}$$

where k_F is the Fermi wave vector. For 3D electron gas $k_F = (\frac{9\pi}{4})^{\frac{1}{3}} \frac{1}{r_s a}$. As mentioned before, we write $r_s = 0$ in the code for the starting case, and

write the known definitions of the noninteracting $g(r)$ and $S(k)$. For the unpolarized electron gas; these functions are:

$$g_F(r) = 1 - \frac{9}{2}\left(\frac{j_1(k_F r)}{k_F r}\right)^2. \tag{4.18}$$

$$S_F(k) = \begin{cases} \frac{3}{4}\frac{k}{k_F} - \frac{1}{16}\frac{k}{k_F}^3 & \text{if } \left|\frac{k}{k_F}\right| \leq 2 \\ 1 & \text{if } \left|\frac{k}{k_F}\right| > 2. \end{cases} \tag{4.19}$$

The fermionic correction function $W_F(r)$ is defined in terms of $g_F(r)$ and $S_F(k)$ as:

$$W_F(k) = -\frac{\hbar^2 k^2}{4m}\left[\frac{(S_F(k)-1)}{S_F(k)}\right]^2 (2S_F(k)+1) + F\left[\frac{\hbar^2}{m}\frac{\nabla^2\sqrt{g_F}}{\sqrt{g_F}}\right]. \tag{4.20}$$

2 Now, the defect function is defined in Eq. (4.2). After taking the Fourier transform of $R(r)$, we find the new $S(k)$:

$$S(k) = \frac{1}{\sqrt{1 + 4\gamma/k^4 + (4/k^2)\left[(m/\hbar^2)W_F(k) - R(k)\right]}}, \tag{4.21}$$

where $\gamma = 4\pi n/a$, and n is the electron density:

$$n = \frac{3}{4\pi}\frac{1}{(r_s a)^3}. \tag{4.22}$$

3 The new $g(r)$ can be found directly as:

$$\begin{aligned} g(r) - 1 = \mathcal{F}^{-1}[S(k)-1] &= \frac{1}{n}\int d^3k \frac{e^{-ik\cdot r}}{(2\pi)^3}[S(k)-1] \\ &= -\frac{4\pi}{3}(r_s a)^3 \int dk \frac{k^2(S-1)}{(2\pi)^3}\int_1^{-1} d(\cos\theta) e^{ikr\cos\theta}\int_0^{2\pi} d\phi \\ &\equiv \frac{2(r_s a)^3}{3\pi}{k_F}^3 \int dk[S(k)-1]k^2\frac{\sin(kr)}{kr} \\ &= \frac{3}{2}\int dk[S(k)-1]k^2 sinc(kr). \end{aligned} \tag{4.23}$$

In the third step of Eq. (4.23), we assigned k/k_F as k.

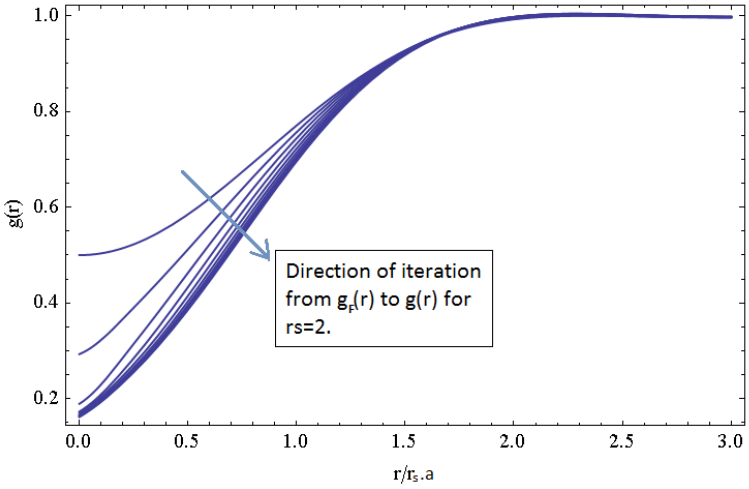

Figure 4.6: The plot of the convergence of the radial distribution function

4 As explained in the 4th item of Sec. 4.1.2, we use mixing for each step and iterate the system until it converges. Fig 4.6 exhibits the convergence of the radial distribution function. To obtain this figure, we initiated the iteration process with the function g_F as defined in Eq. (4.18). To reach the convergence of $g(r)$, we did only 10 iterations, and used the same mixing factor as Eq. (4.7). However, to calculate energy, we have done more iterations to store the data for each r_s value separately, and then interpolated them to take the integral of the potential energy with respect to r_s.

5 We find the potential energy for this case as:

$$\begin{aligned}\frac{V}{N} = V(r_s) &= \frac{n}{2}\int d^3r(g(r)-1)v_c(r) \\ &= \frac{3}{4\pi}\frac{1}{(r_s a)^3}\frac{1}{2}\int r^2 dr\sin\theta d\theta d\phi(g-1)\frac{e^2}{r} \\ &\equiv \left[\frac{3}{r_s}\int r dr(g-1)\right]\text{Ry},\end{aligned} \tag{4.24}$$

where Ry$=\frac{e^2}{2a}$ is the unit of the energy. The total energy per electron is:

$$E_{GS} = \frac{3}{5}\epsilon_F + \frac{1}{{r_s}^2}\int_0^{r_s} dr'_s r'_s V(r'_s), \tag{4.25}$$

where ϵ_F is the Fermi energy. It is found as the following:

$$\begin{aligned}\epsilon_F &= \frac{\hbar^2 k_F^2}{2m} = \frac{\hbar^2}{2m}\left(\frac{9\pi}{4}\right)^{\frac{2}{3}}\frac{1}{r_s^2 a^2} = \frac{\hbar^2}{2m}\left(\frac{9\pi}{4}\right)^{\frac{2}{3}}\frac{1}{r_s^2 a}\frac{me^2}{\hbar^2} \\ &= \frac{e^2}{2a}\left[\frac{1}{2}\left(\frac{9\pi}{4}\right)^{\frac{2}{3}}\right] = \frac{1}{2}\left(\frac{9\pi}{4}\right)^{\frac{2}{3}}\text{Ry}.\end{aligned} \tag{4.26}$$

By placing the Fermi energy, the first term of the ground state energy is found in terms of Ry as:

$$\epsilon_0 = \frac{3}{5}\epsilon_F = \frac{3}{10}\left(\frac{9\pi}{4}\right)^{\frac{2}{3}} \simeq \frac{2.2099}{r_s^2} \tag{4.27}$$

The correlation energy of 3D electron gas:

$$E_C = -E_x + \frac{1}{{r_s}^2}\int_0^{r_s} dr_s' r_s' V(r_s'), \tag{4.28}$$

where E_x is the exchange energy per electron which is found as:

$$E_x = -\frac{3}{4}\frac{e^2 k_F}{\pi} = -\frac{3}{2\pi r_s}\left(\frac{9\pi}{4}\right)^{\frac{1}{3}}\text{Ry} \simeq -\frac{0.916}{r_s}\text{Ry}. \tag{4.29}$$

4.3.3 Results and Analysis

The unpolarized electron gas has only the Coulomb potential among the pair of electrons, and obeys the Pauli exclusion principle. We are starting the iteration process with the noninteracting case functions: $g_F(r)$, and its corresponding $S_F(k)$. In the noninteracting case, electrons are so close to each other that we can neglect the Coulomb interactions. This is the maximum density situation where r_s goes to zero. The pair distribution function can be defined as the probability of finding another particle from our reference particle. Due to the Pauli principle, the probability to find two electrons at the same place is 1/2. That is why in the Fig. 4.7 we see that $g_F(r = 0)$ equals to 0.5 at the highest electron density level. As the density decreases, one can see a decrease in the $g(r)$ value at zero distance. When the system reaches $r_s = 15$, this value becomes almost zero, because it is hard to find two electrons with opposite spins at the same point if they are not in the high density regime.

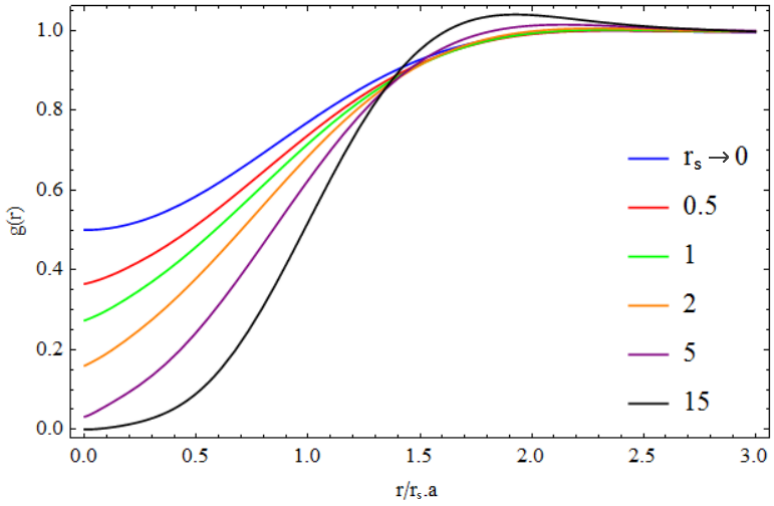

Figure 4.7: Radial distribution function versus $r/r_s a$ for 3D electron gas

The correlation energy results of the 3D electron gas at different densities are given in Table 4.3 along with the results of diffusion Monte Carlo, FHNC, and coupled cluster method calculations. Although, DMC does not give "exact" results for electrons, it is still a very reliable method. The difference between our results and those of Ceperley et al. is typically less than 0.3% that we consider fairly satisfactory for all practical purposes. In addition to this, as you can see in the Table 4.3, we reproduced the results by Kallio et al., and confirmed that this method works very well.

r_s	E_c^{pres}	E_c^{KP}	E_c^{DMC}	E_c^{FHNC}	E_c^{CCM}	E_c^{VMC}
1	-0.1155	-0.1159	-0.1220	-0.1141	-0.1220	-0.1855
2	-0.0869	-0.0870	-0.0902	-0.0859	-0.0904	-0.1050
3	-0.0718	-0.0719	-0.0738	-0.0710	-0.0738	-0.0807
4	-0.0621	-0.0620	-0.0636	-0.0612	-0.0634	-0.0675
5	-0.0550	-0.0549	-0.0563	-0.0541	-0.0560	-0.0585
10	-0.0362	-0.0360	-0.0372	-0.0355	-0.0370	-0.0372
20	-0.0225	-0.0224	-0.0230	-0.0218	-0.0236	-0.0228

Table 4.3: Correlation energy results for the unpolarized electron gas in Ry. KP stands for the results of Kallio et al. [3]. DMC results from Ref. [18], FHNC results from Ref. [19], CCM results from Ref.[20], and VMC results from Ref.[21]. The ground-state energies of Ref.[21] are converted to correlation energies for comparison.

Since we have performed the computation from $r_s = 0$ to $r_s = 1$ by 0.05 steps, we could find accurate results for high density regime, as you can see in the Table 4.4. If we increase the step numbers more, we can find a more accurate result for $r_s = 0.1$; because we are taking an integral from $r_s = 0$ to $r_s = 0.1$, and increasing steps provides a better interpolation of the data. Table 4.4 shows that for small r_s, our numerical results agree closely with the field theory results [22]. Since field theoretical approach works at high electron density regime, we can compare our small r_s results with it.

r_s	E_c^{pres}	E_c^{KP}	E_c^{BL}
0.1	-0.223	-0.229	-0.237
0.2	-0.190	-0.193	-0.194
0.3	-0.171	-0.172	-0.169
0.4	-0.157	-0.158	-0.151
0.5	-0.147	-0.147	-0.137
0.6	-0.138	-0.138	-0.126
0.7	-0.131	-0.132	-0.116
0.8	-0.125		
0.9	-0.120		

Table 4.4: Correlation energy results for the unpolarized electron gas in high density range in Ry. The correlation energies E_C^{BL} are calculated from $E_C^{BL} = 0.0622 \ln r_s - 0.094$, Ref. [22], and E_C^{KP} are the results of Kallio et al. [3].

4.4 2D Spin Unpolarized Electron Liquid

4.4.1 Definition

The two-dimensional electron gas model can be realized in semi-conductor interfaces (GaAs-$Ga_{1-x}Al_xAs$) or at the interface of a metal oxide and a semiconductor (MOS) [23]. The electron liquid in such interfaces has important characteristics such that they display the quantum Hall effect at very low temperatures and in the presence of a strong and uniform magnetic field. Thereby, the theoretical

investigation of the behavior of 2D electron liquid has significance owing to its intriguing, complex behavior and its several applications in many-body physics.

In this section, we present our results of the statistical properties for uniform 2D electron gas at zero temperature with no magnetic field.

4.4.2 The Algorithm

In this part, the algoritm we used for 2D electron gas is explained step by step:

1 At first, we make all the variables dimensionless:

$$r/r_s a \to r, \qquad k/k_F \to k \tag{4.30}$$

where k_F is the Fermi wave vector. For 2D electron gas $k_F = \frac{\sqrt{2}}{r_s a}$. As mentioned before, we write $r_s = 0$ in the code for the starting case, and write the known definitions of the noninteracting $g(r)$ and $S(k)$. For the unpolarized 2D electron gas; these functions are:

$$g_F(r) = 1 - \frac{1}{2}\left(\frac{2J_1(k_F r)}{k_F r}\right)^2. \tag{4.31}$$

$$S_F(k) = \begin{cases} \frac{2}{\pi}\sin^{-1}\left(\frac{k}{2k_F}\right) + \frac{k}{2k_F}\sqrt{1-(\frac{k}{2k_F})^2} & \text{if } \frac{k}{k_F} \leq 2 \\ 1 & \text{if } \frac{k}{k_F} > 2. \end{cases} \tag{4.32}$$

By using the definitions of $g_F(r)$ and $S_F(k)$, we can find the fermionic correction term $W_F(r)$ as:

$$W_F(k) = -\frac{\hbar^2 k^2}{4m}\left[\frac{(S_F(k)-1)}{S_F(k)}\right]^2 (2S_F(k)+1) + F\left[\frac{\hbar^2}{m}\frac{\nabla^2\sqrt{g_F}}{\sqrt{g_F}}\right]. \tag{4.33}$$

2 The defect function can be calculated by Eq. (4.2). After taking the Fourier transform of $R(r)$, we find the new $S(k)$:

$$S(k) = \frac{1}{\sqrt{1 + 4\gamma_{2d}/k^3 + (4/k^2)\left[(m/\hbar^2)W_F(k) - R(k)\right]}}, \tag{4.34}$$

where $\gamma_{2d} = 2\pi n/a$, and n is the electron density:

$$n = \frac{1}{\pi(r_s a)^2}. \tag{4.35}$$

3 The new $g(r)$ can be found directly as:

$$\begin{aligned} g(r) - 1 &= \frac{1}{n}\int d^2k \frac{e^{-ik\cdot r}}{(2\pi)^2}[S(k) - 1] \\ &= \pi r_s^2 a^2 \frac{1}{(2\pi)^2}\int dk(S-1)k\int_0^{\pi} d\theta e^{ikr\cos\theta} \\ &\equiv \int dk[S(k) - 1]kJ_0(kr). \end{aligned} \tag{4.36}$$

In the third step of the Eq. (4.36), we assigned k/k_F as k.

4 We inserted new $g(r)$ into the defect function $R(r)$ which is defined in Eq. (4.2). We did the iteration process until the pair distribution function converges for each r_s value. In the Fig. 4.8, you can see the convergence of the radial distribution function. Each point on the plot stands for the integral value $\int dr|g_{after}(r) - g_{before}(r)|$ calculated after each iteration.

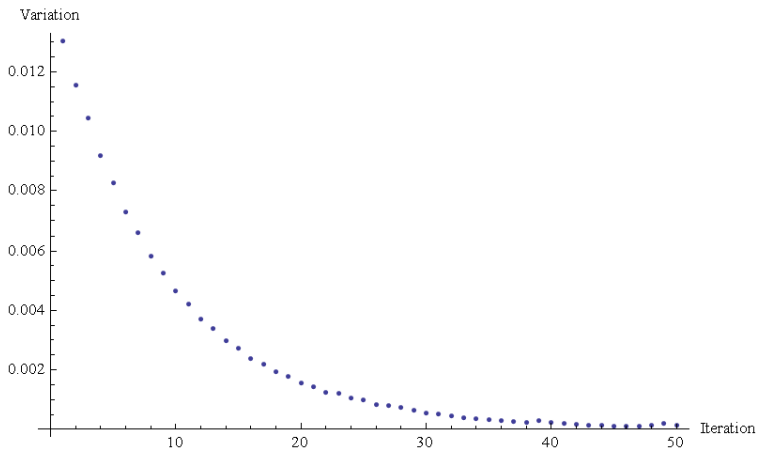

Figure 4.8: The plot of the convergence of the radial distribution function for 2D electron gas

5 The potential energy for each r_s value can be calculated by Eq. (4.16). After taking interpolation of the function $V(r_s)$, we can find the ground-state energy:

$$E_{GS} = \frac{\epsilon_F}{2} + \frac{1}{{r_s}^2}\int_0^{r_s} dr'_s r'_s V(r'_s), \tag{4.37}$$

where ϵ_F is the Fermi energy. It is found as the following:

$$\begin{aligned}\epsilon_F &= \frac{\hbar^2 k_F^2}{2m} = \frac{\hbar^2}{2m}\frac{2}{(r_s a)^2} = \frac{\hbar^2}{2m}\frac{2}{(r_s^2 a)}\frac{me^2}{\hbar^2} \\ &= \frac{e^2}{2a}\left[\frac{2}{r_s^2}\right] = \frac{2}{r_s^2}\text{Ry}.\end{aligned} \tag{4.38}$$

By placing the Fermi energy, the first term of the ground state energy is found in terms of Ry as:

$$\epsilon_0 = \frac{\epsilon_F}{2} = \frac{1}{r_s^2}. \tag{4.39}$$

The correlation energy of 2D electron gas:

$$E_C = -E_x + \frac{1}{{r_s}^2}\int_0^{r_s} dr'_s r'_s V(r'_s), \tag{4.40}$$

where E_x is the exchange energy per electron which is calculated as:

$$E_x = -\frac{4}{3}\frac{e^2 k_F}{\pi} = -\frac{8\sqrt{2}}{3\pi r_s}\text{Ry} \simeq -\frac{1.200}{r_s}\text{Ry}. \tag{4.41}$$

4.4.3 Results and Analysis

Our results of pair correlation function $g(r)$ for 2D paramagnetic electron gas for different r_s are presented in Fig. 4.9. As we expected, the pair distribution function at zero distance between the electrons approaches to zero as the density of electrons decreases. In Sec. 4.2.3, we have stated that three-body correlations are more important for 2D systems than 3D systems. However, by using the simple and effective method by Kallio et al. for 2D, we could find good results for the 2D unpolarized electron gas. To show this in a clear way, we compared our present result $g(r)$ with the FHNC result in the Fig. 4.10. Although the result by Asgari et al. includes triplet correlations, it is obvious that there is not a significant difference between them.

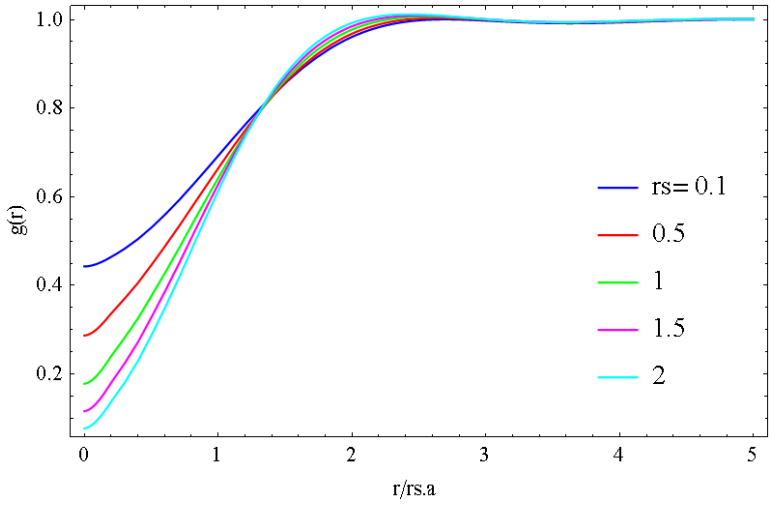

Figure 4.9: Radial distribution function of 2D electron gas at several densities for unpolarized 2D electron gas.

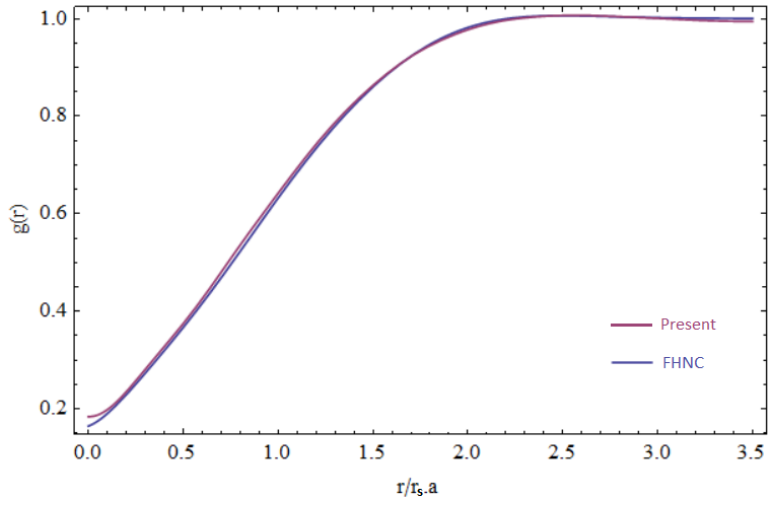

Figure 4.10: The pair distribution function $g(r)$ of the 2D electron gas at $r_s = 1$ in the paramagnetic state, as a function of distance r (in units of $r_s a$). The present results, shown in red, are compared with FHNC data by Asgari et al. [24], shown in blue.

Bibliography

[1] G. F. Giuliani and G. Vignale, *Quantum Theory of the Electron Liquid*. Cambridge University Press, 2008.

[2] A. Fabrocini, S. Fantoni, and E. Krotscheck, *Introduction to Modern Methods of Quantum Many-Body Theory and Their Applications*. World Scientific Publishing, 2002.

[3] A. Kallio and J. Piilo, "Novel analytic calculation of electron gas properties," *Physical Review Letters*, vol. 77, no. 20, 1996.

[4] G. D. Mahan, *Many Particle Physics*. Physics of Solids and Liquids, 2002.

[5] J. M. J. V. Leeuwen, J. Groeneveld, and J. D. Boer, "New method for the calculation of the pair correlation function. I," *Physica*, vol. 25, pp. 663–667, 1959.

[6] S. Fantoni and S. Rosati, "Automatic classification for pathological prostate images based on fractal analysis," *Nuovo Cimento A*, vol. 20, no. 179, 1974.

[7] A. Kallio, V. Apaja, and S. Pöykkö, "Spectator fermion binding of bosons," *Physica B*, vol. 210, no. 472-478, 1995.

[8] V. Apaja, J. Halinen, V. Halonen, E. Krotscheck, and M. Saarela, "Charged-boson fluid in two and three dimensions," *Physical Review B*, vol. 55, no. 19, 1997.

[9] B. W. Ninham, "Charged Bose gas in astrophysics," *Physics Letters*, vol. 4, pp. 278–279, 1963.

[10] J. P. Hansen, B. Jancovici, and D. Schiff, "Phase diagram of a charged Bose gas," *Physical Review Letters*, vol. 29, no. 991, 1972.

[11] V. L. Ginzburg, "Superfluidity and superconductivity in the universe," *Journal of Statistical Physics*, vol. 1, 1969.

[12] S. Moroni, S. Conti, and M. P. Tosi, "Monte carlo simulations of the charged boson fluid at t=0," *Physical Review B*, vol. 53, no. 9688, 1996.

[13] R. T. Hock-Kee Sim and F. Y. Wu, "Ground-state energy of charged quantum fluids in two dimensions," *Physical Review B*, vol. 34, no. 7123, 1986.

[14] A. Gold, "Local-field correction of the charged Bose condensate for two and three dimensions," *Zeitschrift fr Physik B Condensed Matter*, vol. 89, pp. 1–10, 1992.

[15] M. Gell-Man and K. A. Brueckner, "Correlation energy of an electron gas at high density," *Physical Review*, vol. 106, no. 2, 1956.

[16] D. Ceperley, "Condensed-matter physics: Return of the itinerant electron," *Nature*, vol. 397, no. 386, 1999.

[17] N. H. March, *Electron Correlations in the Solid State*. Imperial College Press, London, 1999.

[18] D. M. Ceperley and B. J. Alder, "Ground state of the electron gas by a stochastic method," *Physical Review B*, vol. 45, no. 566, 1980.

[19] L. J. Lantto, "Variational theory of multicomponent quantum fluids: An application to positron-electron plasmas at t=0," *Physical Review B*, vol. 36, no. 5160, 1987.

[20] K. Emrich and J. G. Zabolitzky, "Electron correlations in the Bogoljubov coupled-cluster formalism," *Physical Review B*, vol. 30, no. 2049, 1984.

[21] D. Ceperley, "Ground state of the fermion one-component plasma: A Monte Carlo study in two and three dimensions," *Physical Review B*, vol. 18, no. 7, pp. 3126–3138, 1978.

[22] R. F. Bishop and K. H. Lührmann, "Electron correlations: I. ground-state results in the high-density regime," *Physical Review B*, vol. 17, no. 3757, 1978.

[23] B.Tanatar and D. M. Ceperley, "Ground state of the two-dimensional electron gas," *Physical Review B*, vol. 39, no. 8, 1988.

[24] R. Asgari, B. Davoudi, and M. Tosi, "Analytic theory of correlation energy and spin polarization in the 2d electron gas," *Solid State Communications*, vol. 131, pp. 301–305, 2004.

Appendix A

Minimization of the Energy

As it is explained in Sec. 3.2, we will take functional derivative of the total energy per particle expression (A.1) with respect to the function $G(r)$. Since we want to find the ground-state energy by a variational method, we equate the derivative of the energy expression to zero in order to minimize the energy.

We have done the functional derivatives step by step to reach the iterative scheme of the HNC/0 method. First, we write the definition of total energy per particle in its open form:

$$\begin{aligned} e = & \frac{n}{2}\int dr g(r)v(r) - \frac{\hbar^2}{8m}\frac{1}{(2\pi)^3 n}\int dk k^2 \frac{(S-1)^3}{S} \\ & - \frac{n}{2}\frac{\hbar^2}{4m}\int dr g(r)\nabla^2 \ln g(r). \end{aligned} \tag{A.1}$$

As stated in Sec. 3.2 we take the functional derivative with respect to $\sqrt{g(r)}$ which is denoted as $G(r)$. First, we start from the first term of the energy expression. The integral part of this term can be defined as $F_1 = \int dr G^2(r)\nu(r)$. The functional derivative of an equation is defined by the following formula:

$$\int \frac{\delta F}{\delta n(r)}\phi(r)dr = \int \left(\frac{\partial f}{\partial n} - \nabla \frac{\partial f}{\partial \nabla n}\right)\phi(r)dr, \tag{A.2}$$

where $F = \int dr f(r)$. Here, $F = F_1$, and $f(r) = G^2(r)v(r)$. So we can take the

functional derivative of the F_1 function:

$$\delta F_1 = \delta\left[\int drG^2 v(r)\right] = \int\left[\frac{\partial}{\partial G}(G^2\nu(r)) - \nabla\overset{zero}{\frac{\partial}{\partial\nabla G}}\left(G^2\nu(r)\right)\right](\delta G)dr, \quad \text{(A.3)}$$

$$\delta F_1 = \int 2G(r)\nu(r)(\delta G)dr \Rightarrow \frac{\delta F_1}{\delta G} = 2G\nu(r). \quad \text{(A.4)}$$

Then the functional derivative of the first term is found as:

$$\frac{\delta}{\delta G}\left(\frac{n}{2}\int drG^2(r)\nu(r)\right) = \frac{n}{2}\frac{\delta F_1}{\delta G} = \frac{n}{2}2G\nu(r) = nG(r)\nu(r). \quad \text{(A.5)}$$

Now, we can move our calculation to the second term of the energy per particle expression, which is:

$$-\frac{\hbar^2}{8m}\frac{1}{(2\pi)^3 n}\int dkk^2\frac{(S-1)^3}{S}, \quad \text{(A.6)}$$

where its integral part is denoted as F_2. Now, we take the functional derivative of is as follows:

$$\begin{aligned}\delta F_2 &= \delta\left[\int dkk^2\frac{(S-1)^3}{S}\right] \\ &= \int\left[\frac{\partial}{\partial S}\left(k^2\frac{(S-1)^3}{S}\right) - \nabla\frac{\partial}{\partial\nabla S}\left(k^2\frac{(S-1)^3}{S}\right)\right](\delta S)dk \quad \text{(A.7)} \\ &= \int k^2\frac{\partial}{\partial S}\frac{(S-1)^3}{S}\delta S dk.\end{aligned}$$

In this integral the partial derivative with respect to $S(k)$ is found as:

$$\frac{\partial}{\partial S}\left[\frac{(S-1)^3}{S}\right] = \left(\frac{S-1}{S}\right)^2(2S+1). \quad \text{(A.8)}$$

By placing Eq. (A.8) into (A.7) we can find;

$$\delta F_2 = \int k^2 dk\left(\frac{(S-1)^2}{S}\right)(2S+1)\delta S, \quad \text{(A.9)}$$

$$\delta(S-1) = \delta(G^2-1). \quad \text{(A.10)}$$

In Eq. (A.9), δS can be found by using the Fourier transform relationship between $S-1$ and $g-1$. Thus;

$$S-1 = \widetilde{G^2-1} \quad \text{(A.11)}$$

$$\delta(S-1) = \delta(\widetilde{G^2-1}) \quad \text{(A.12)}$$

$$\delta S = 2\widetilde{G\delta G} \tag{A.13}$$

By substituting Eq. (A.13) into the Eq. (A.9):

$$\delta F_2 = \int k^2 dk \left(\frac{S-1}{S}\right)^2 (2S+1) 2\widetilde{G\delta G} \tag{A.14}$$

Now, we can write the functional derivative of the second term of the energy expression (A.6) by inserting Eq. (A.14) to it:

$$\frac{1}{(2\pi)^3 n} \int dk \left(-\frac{\hbar^2 k^2}{4m}(2S+1)(\frac{S-1}{S})^2\right) \widetilde{G\delta G} \tag{A.15}$$

To solve Eq. (A.15), we will use Parseval's identity:

$$n \int A(r)B(r)dr = \frac{1}{(2\pi)^3 n} \int dk \widetilde{A(k)}\widetilde{B(k)}, \tag{A.16}$$

where $\widetilde{A(k)} = -\frac{\hbar^2 k^2}{4m}(2S+1)(\frac{S-1}{S})^2 = \widetilde{w(k)}$, and $\widetilde{B(k)} = \widetilde{G\delta G}$. Therefore, the functional derivative of the second term with respect to $G(r)$ can be found as:

$$\frac{\delta}{\delta G}\left(-\frac{\hbar^2}{8m}\frac{1}{(2\pi)^3 n}\int dk k^2 \frac{(S-1)^3}{S},\right) = n w_0(r) G(r) \tag{A.17}$$

The integral part of the third term of the Eq. (A.1) is denoted as F_3:

$$F_3[G] = \int dr(\nabla G)^2 \Rightarrow F_3[G+\epsilon h] = \int dr(\nabla G(r) + \epsilon h'(r))^2 \tag{A.18}$$

As $\epsilon \to 0$ the functional derivative of F_3:

$$\delta F_3 = \frac{d}{d\epsilon}\mathcal{F}[G+\epsilon h] = \frac{d}{d\epsilon}\int dr(\nabla G + \epsilon h')^2 \tag{A.19}$$

The derivative with respect to ϵ is found as:

$$\frac{d}{d\epsilon}(\nabla G + \epsilon h')^2 = \frac{d}{d\epsilon}(\nabla G)^2 + 2\nabla G \epsilon h' + \epsilon^2 h'^2 = 2\nabla G h' \tag{A.20}$$

Then we put the Eq. (A.20) into (A.19):

$$\delta F_3 = \int dr 2\nabla G \nabla h \tag{A.21}$$

Now, we apply integration by parts:

$$\int dr \nabla G \nabla h = G \cdot h - \int h \nabla^2 G dr = -\int h \nabla^2 G dr \tag{A.22}$$

So, δF_3 is:

$$\delta F_3 = -2 \int h \nabla^2 G dr. \tag{A.23}$$

Then, we can write the functional derivative of F_3 with respect to $G(r')$:

$$\frac{\delta F_3[G]}{\delta G(r')} = -2 \int \nabla^2 G \delta(r - r') = -2\nabla^2 G. \tag{A.24}$$

Thus, we can place Eq. (A.24) into the third term, and then take its functional derivative with respect to G:

$$\frac{\delta}{\delta G}\left(-\frac{n}{2}\frac{\hbar^2}{4m}\int dr g(r)\Delta \ln g(r).\right) = -2\frac{\hbar^2}{2m} n\nabla^2 G = -\frac{\hbar^2}{m} n\nabla^2 G(r). \tag{A.25}$$

Now, we found the functional derivatives of all the terms of the energy per particle expression given in Eq. (A.1). If place our results for 1st, 2nd and 3rd terms of Eq. (A.1), and equate it to 0 for minimization of the energy, we find:

$$\begin{aligned} \frac{\delta e}{\delta G} = nG(r)v_c(r) + nw_0(r)G(r) - \frac{\hbar^2}{m} n\nabla^2 G(r) = 0 \\ n\left(-\frac{\hbar^2}{m}\nabla^2 G + v_c(r) + w_0(r)\right) G(r) = 0 \\ \left(-\frac{\hbar^2}{m}\nabla^2 G + v_c(r) + w_0(r)\right) G(r) = 0, \end{aligned} \tag{A.26}$$

where $G(r) = \sqrt{g(r)}$. This is the main differential equation of the hypernetted chain method. It is also called Schrödinger-like equation, because the function $G(r)$ acts like the probability amplitude of this zero energy equation. This is explained in Sec. 3.4.

Appendix B

The Equivalence of the Methods

From the Eq. (3.22), the main differential equation is:

$$\frac{-\hbar^2}{m}\nabla^2\psi + (W_B(r) + v_c(r))\psi = 0, \tag{B.1}$$

where $\psi = \sqrt{g}$. Here, we will show the equivalence of the HNC/0 iterative schemes which are presented by Kallio et al. and Fantoni. By this equivalence, we will find how γ term is found as $4\pi n/a$ for 3D electron gas by Kallio, so that we can convert it for 2D electron gas case.

The fluctuations of a function can cause crucial problems while taking its integral. Since Kallio did the iteration on a defect function $R(r)$, his method eliminates this problem, and we can find better results. That's why we need to find γ for the 2D electron gas.

First we reorganize the highly nonlinear differential equation defined in Eq. (B.1):

$$\frac{-\hbar^2}{m}\frac{\nabla^2\psi}{\psi} + W_B + v_c = 0. \tag{B.2}$$

Then, we insert the definitions of $v_c(r)$ and $W_B(r)$ into the Eq. (B.2), and multiply both sides by $m/\hbar^2$:

$$\frac{\nabla^2\psi}{\psi} + \frac{me^2}{\hbar^2 r} = \mathcal{F}\left[\frac{k^2}{4}\left(\frac{S-1}{S}\right)^2 (2S+1)\right]. \tag{B.3}$$

Then, we take inverse Fourier transform of both sides:

$$\frac{k^2}{4}\left(\frac{S-1}{S}\right)^2 (2S+1) = \mathcal{F}^{-1}\left[\frac{-\nabla^2\psi}{\psi} + \frac{me^2}{\hbar^2 r}\right]. \tag{B.4}$$

Now we put Eq. (3.27) into (B.4):

$$\frac{k^2}{4}\left(\frac{S-1}{S}\right)^2 (2S+1) = \mathcal{F}^{-1}\left[-\frac{1}{2}\nabla^2(g-1) - R(r) + \frac{me^2}{\hbar^2 r}\right]. \tag{B.5}$$

Here, $\mathcal{F}^{-1}[\nabla^2(g-1)] = (-k^2)(S-1)$ due to the Fourier transform relation between $g(r)-1$ and $S(k)-1$. So, we insert this into Eq. (B.5). After multiplying both sides by $4/k^2$, we find:

$$2S - 3 + \frac{1}{S^2} = (S-1) - \frac{4}{k^2}R(k) + \frac{4me^2}{\hbar^2 k^2}\mathcal{F}\left[\frac{1}{r}\right]. \tag{B.6}$$

Here; $\hbar^2/me^2 = a$ is the Bohr radius and $\mathcal{F}[1/r] = 4\pi n/k^2$ if we take the Fourier transform in 3D analytically. Reorganizing the equation we find:

$$\frac{1}{S^2} = 1 - \frac{4}{k^2}R(k) + \frac{4}{ak^2}\mathcal{F}\left[\frac{1}{r}\right] = 1 - \frac{4}{k^2}R(k) + \frac{4}{ak^2}\left(\frac{4\pi n}{k^2}\right), \tag{B.7}$$

$$S(k) = \left(1 - \frac{4}{k^2}R(k) + \frac{16\pi n}{ak^4}\right)^{-1/2}. \tag{B.8}$$

This is the main iterative formula which is also given in Eq. (3.28). From their equivalence, one can find:

$$\frac{16\pi n}{ak^4} = \frac{4\gamma}{k^4}. \tag{B.9}$$

So, here we confirmed that $\gamma = 4\pi n/a$ for 3D electron gas. To find 2D γ, we return the Eq. (B.6) and define the Fourier transform for 2D system as:

$$\mathcal{F}\left[\frac{1}{r}\right] = \frac{2\pi n}{k} \tag{B.10}$$

where $n = 1/\pi(r_s a)^2$. By placing Eq. (B.10) into (B.6), we find the equation

$$\frac{1}{S^2} = 1 - \frac{4}{k^2}R(k) + \frac{4}{ak^2}\frac{2\pi n}{k} \tag{B.11}$$

So, the static structure factor is:

$$S = \left(1 - \frac{4}{k^2}R(k) + \frac{8\pi n}{ak^3}\right)^{-1/2} = \left(1 - \frac{4}{k^2}R(k) + \frac{4\gamma_{2d}}{k^3}\right)^{-1/2} \tag{B.12}$$

where $\gamma_{2d} = 2\pi n/a$.

Appendix C

The Code

In this chapter, I share the Mathematica code for 2D and 3D Bose and electron liquid systems. The algorithms are explained in detail in Chapter 4. The choice of range of integrals, interpolation, and the mixing ratio may need to be adapted for different rs values and/or different cases.

C.1 3D Electron Gas

Below is the Mathematica code for the 3D spin unpolarized electron gas calculations.

```
(*Beginning of constants and function definitions*)
itercnt = 200;(*Number of iterations*)
rs = 1; (*Assign an initial value for rs*)
gf[r_] := 1 - (((9/2)*SphericalBesselJ[1, kfr[r]]^2)/(kfr[r]^2));
Sf[k_] := N[If[k < 2, (3*k)/4 - (k^3)/16, 1]];
kfr[r_] := (((9*Pi)/4)^(1/3))*r;
kokgf[r_] := Sqrt[gf[r]]
kokgr[r_] := Sqrt[gr[r]]
Lapgminus[r_] := Derivative[2][gr][r] + (2*Derivative[1][gr][r])/r;
```

```
Lapkokgf[r_] :=
  Derivative[2][kokgf][r] + (2*Derivative[1][kokgf][r])/r;
Lapkokgr[r_] :=
  Derivative[2][kokgr][r] + (2*Derivative[1][kokgr][r])/r;
ad[r_] := (Lapkokgf[r]/kokgf[r]) - (Lapkokgr[r]/kokgr[r]) + (1/2)*
    Lapgminus[r];
adFT0[r_, k_] := (r^2)*ad[r]*Sinc[k*kfr[r]];
add[k_] := 3*
   NIntegrate[adFT0[r, k], {r, 0, 49.91},
    Method -> {"GlobalAdaptive", "SymbolicProcessing" -> 0}];
Smin[k_] := ((1 + ((4/(9*Pi))^(4/3))*(12*
           rs/(k^4)) + ((2*Sf[k] +
            1)*(((Sf[k] - 1)/
              Sf[k])^2)) + ((((4*((4/(9*Pi))^(2/3))))/(k^2))*
          add[k]))^(-1/2)) - 1;
SminFT0[k_, r_] := (k^2)*Sinter[k]*Sinc[k*kfr[r]];
smin[r_] := (3/2)*
  NIntegrate[SminFT0[k, r], {k, 0, 49.91},
   Method -> {"GlobalAdaptive", "SymbolicProcessing" -> 0}]
(*End of definitions*)

(*The block below represents a single iteration. It takes a trial
function as an input, calculates S(k) and using that S(k) (sinter),
calculated g(r) (ginter). err is the variation between the trial
function and the calculated function. Output function gout is the
mixture of gtrial and ginter*)
ErrorCalcgr[grtrial_] := Block[{},
  gr = grtrial;
  Sinter = Quiet[FunctionInterpolation[Smin[k], {k, 0.01, 49.91}]];
  ginter =
   Quiet[FunctionInterpolation[(1 + smin[r]), {r, 0.01, 49.91}]];
  (*to reduce the fluctuations calculated g(r) is mixed with the
trial function*)
```

```
  fif[r_] := ((ginter[r]) + (9*grtrial[r]))/10;
  gout = Interpolation[
    Transpose[{Table[n, {n, 0.01, 49.91, 0.2}],
      Table[fif[n], {n, 0.01, 49.91, 0.2}]}]];
  err = NIntegrate[Abs[gout[r] - grtrial[r]], {r, 0, 12}];
  Return[{err, gr, gout, ginter}];
  ]
(*The block below does the iterations for a given rs and collects the
result of each iteration*)
Rstogr[rsn_] := Block[{},
   iter = {};
   Do[
    rs = rsn;
    err1 = ErrorCalcgr[gr];
    iter = Append[iter, err1];
    Print[ToString[n] <> "Error: " <> ToString[Part[iter, n, 1]]];
    gr = Part[iter, n, 3];
    If [err < 0.000001, Break[Null, Do]]
    , {n, itercnt}]; iter];
```

C.2 3D Charged Bose Gas

Below is the Mathematica code for the 3D Charged boson gas calculations.

```
itercnt = 250;
rs = 0;
gf[r_] := 1;
Sf[k_] := 1;
kfr[r_] := (((9*Pi)/4)^(1/3))*r;
kokgr[r_] := Sqrt[gr[r]];
Lapgminus[r_] := Derivative[2][gr][r] + (2*Derivative[1][gr][r])/r;
Lapkokgr[r_] :=
```

```
  Derivative[2][kokgr][r] + (2*Derivative[1][kokgr][r])/r;
ad[r_] := (Lapkokgr[r]/kokgr[r]) - (1/2)*Lapgminus[r];
adFT0[r_, k_] := (r^2)*ad[r]*Sinc[k*kfr[r]];
add[k_] := 3*
   NIntegrate[adFT0[r, k], {r, 0, 10},
    Method -> {"GlobalAdaptive", "SymbolicProcessing" -> 0}];
Smin[k_] := ((1 + ((4/(9*Pi))^(4/3))*(12*
          rs/(k^4)) - ((((4*((4/(9*Pi))^(2/3))))/(k^2))*add[k]))^(-1/
       2)) - 1;
SminFT0[k_, r_] := (k^2)*Sinter[k]*Sinc[k*kfr[r]];
gmin[r_] := (3/2)*
  NIntegrate[SminFT0[k, r], {k, 0, 40},
   Method -> {"GlobalAdaptive", "SymbolicProcessing" -> 0}]
gr = gf;

ErrorCalcgr[grtrial_] := Block[{},
  gr = grtrial;
  Sinter = Quiet[FunctionInterpolation[Smin[k], {k, 0, 40}]];
  ginter = Quiet[FunctionInterpolation[(1 + gmin[r]), {r, 0, 40}]];
  fif[r_] := ((ginter[r]) + (2*grtrial[r]))/3;
  gout = Interpolation[
    Transpose[{Table[n, {n, 0.01, 40, 0.1}],
      Table[fif[n], {n, 0.01, 40, 0.1}]}]];
  err = NIntegrate[Abs[gout[r] - grtrial[r]], {r, 0, 12}];
  Return[{err, gr, gout, ginter}];
  ]
Rstogr[rsn_] := Block[{},
   iter = {};
   Do[
    rs = rsn;
    err1 = ErrorCalcgr[gr];
    iter = Append[iter, err1];
    Print[ToString[n] <> "Error: " <> ToString[Part[iter, n, 1]]];
```

```
    gr = Part[iter, n, 3];
    If [err < 0.0000001, Break[Null, Do]]
    , {n, itercnt}];
   iter];
```

C.3 2D Charged Bose Gas

Below is the Mathematica code for the 2D Charged boson gas calculations.

```
itercnt = 150;
rs = 0;
gf[r_] := 1;
gr = gf;
grminus[r_] := gr[r] - 1;
Sf[k_] := 1
kfr[r_] := Sqrt[2]*r;
kokgr[r_] := Sqrt[gr[r]];
Lapgminus[r_] :=
  Derivative[2][grminus][r] + (Derivative[1][grminus][r])/r;
Lapkokgr[r_] := Derivative[2][kokgr][r] + (Derivative[1][kokgr][r])/r;
R[r_] := (Lapkokgr[r]/kokgr[r]) - (1/2)*Lapgminus[r];
RFT0[r_, k_] := r*R[r]*Sinc[k*kfr[r]];
Rk[k_] :=
  2*NIntegrate[RFT0[r, k], {r, 0, 99.91},
    Method -> {"GlobalAdaptive", "SymbolicProcessing" -> 0}];
Smin[k_] := ((1 + (Sqrt[8]*rs/(k^3)) - ((2/(k^2))*Rk[k]))^(-1/2)) - 1;
SminFT0[k_, r_] := k*Sinter[k]*Sinc[k*kfr[r]];
gmin[r_] :=
 NIntegrate[SminFT0[k, r], {k, 0, 99.91},
  Method -> {"GlobalAdaptive", "SymbolicProcessing" -> 0}]

ErrorCalcgr[grtrial_] := Block[{},
```

```
  gr = grtrial;
  Sinter =
   Interpolation[
    Transpose[{Table[n, {n, 0.01, 99.91, 0.1}],
      Table[Smin[n], {n, 0.01, 99.91, 0.1}]}]];
  ginter =
   Interpolation[
    Transpose[{Table[n, {n, 0.01, 99.91, 0.1}],
      Table[1 + gmin[n], {n, 0.01, 99.91, 0.1}]}]];
  fif[r_] := ((ginter[r]) + (19*grtrial[r]))/20;
  gout = Interpolation[
    Transpose[{Table[n, {n, 0.01, 99.91, 0.1}],
      Table[fif[n], {n, 0.01, 99.91, 0.1}]}]];
  err = NIntegrate[Abs[ginter[r] - grtrial[r]], {r, 0, 99.91}];
  Return[{err, gr, gout, ginter}];
  ]

Rstogr[rsn_] := Block[{},
   iter = {};
   Do[
    rs = rsn;
    err1 = ErrorCalcgr[gr];
    iter = Append[iter, err1];
    Print[ToString[n] <> "Error: " <> ToString[Part[iter, n, 1]]];
    gr = Part[iter, n, 3];
    If [err < 0.000000386, Break[Null, Do]]
    , {n, itercnt}];
   iter];
```

C.4 2D Electron Gas

Below is the Mathematica code for the 2D spin unpolarized electron gas calculations.

```
itercnt = 120;
rs = 0;
gf[r_] := 1 - ((1/2)*(2*BesselJ[1, kfr[r]]/kfr[r])^2);
Sf[k_] := N[
    If[k <= 2, (2/Pi)*(ArcSin[k/2] + (k/2)*Sqrt[1 - ((k/2)^2)]), 1]];
kfr[r_] := Sqrt[2]*r;
kokgf[r_] := Sqrt[gf[r]]
kokgr[r_] := Sqrt[gr[r]]
Lapgminus[r_] := Derivative[2][gr][r] + (Derivative[1][gr][r])/r;
Lapkokgf[r_] := Derivative[2][kokgf][r] + (Derivative[1][kokgf][r])/r;
Lapkokgr[r_] := Derivative[2][kokgr][r] + (Derivative[1][kokgr][r])/r;
ad[r_] := (Lapkokgf[r]/kokgf[r]) - (Lapkokgr[r]/kokgr[r]) + (1/2)*
     Lapgminus[r];
adFT0[r_, k_] := r*ad[r]*BesselJ[0, k*kfr[r]];
add[k_] := 2*
    Quiet[NIntegrate[adFT0[r, k], {r, 0, 15.01},
      Method -> {"GlobalAdaptive", "SymbolicProcessing" -> 0}]];
Smin[k_] := ((1 + ((Sqrt[8])*
          rs/(k^3)) + ((2*Sf[k] +
            1)*(((Sf[k] - 1)/Sf[k])^2)) + (2/(k^2))*add[k])^(-1/2)) - 1;
SminFT0[k_, r_] := k*Sinter[k]*BesselJ[0, k*kfr[r]];
Gmin[r_] :=
 Quiet[NIntegrate[SminFT0[k, r], {k, 0, 15.01},
   Method -> {"GlobalAdaptive", "SymbolicProcessing" -> 0}]]
gr = gf;
ErrorCalcgr[grtrial_] := Block[{},
  gr = grtrial;
  Sinter =
```

```
    Interpolation[
     Transpose[{Table[n, {n, 0.01, 15.01, 0.1}],
       Table[Smin[n], {n, 0.01, 15.01, 0.1}]}]];
   ginter =
    Interpolation[
     Transpose[{Table[n, {n, 0.01, 15.01, 0.1}],
       Table[1 + Gmin[n], {n, 0.01, 15.01, 0.1}]}]];
   err = NIntegrate[Abs[ginter[r] - grtrial[r]], {r, 0, 10}];
   fif[r_] := (ginter[r] + (9*(grtrial[r])))/10;
   gout = Interpolation[
     Transpose[{Table[n, {n, 0.01, 15.01, 0.1}],
       Table[fif[n], {n, 0.01, 15.01, 0.1}]}]];
   Return[{err, gr, gout, ginter}];
   ]

Rstogr[rsn_] := Block[{},
    iter = {};
    Do[
     rs = rsn;
     err1 = ErrorCalcgr[gr];
     iter = Append[iter, err1];
     Print[ToString[n] <> "Error: " <> ToString[Part[iter, n, 1]]];
     gr = Part[iter, n, 3];
     If [Part[iter, n, 1] < 0.00000496273, Break[Null, Do]]
     , {n, itercnt}];
    iter];
```